

JAN 12 2001

AFRL-SR-BL-TR-01-

## REPORT DOCUMENTATION PAGE

9  
of  
10

Public reporting burden for this collection of information is estimated to average 1 hour per response, including the time for reviewing existing information, gathering new information, and maintaining the data needed, and completing and reviewing the collection of information. Send comments regarding this burden estimate or any other aspect of this collection of information, including suggestions for reducing this burden, to Washington Headquarters Services, Directorate for Information Operations and Reports, 1204, Arlington, VA 22202-4302, and to the Office of Management and Budget, Paperwork Reduction Project (0704-0188), Washington, DC 20503.

1. AGENCY USE ONLY (Leave blank)		2. REPORT DATE 1 January 2001		3. REPORT TYPE AND DATES COVERED Final Technical Report (1 July 94 - 30 June 97)	
4. TITLE AND SUBTITLE Templated Grain Growth of Single Crystal-Like Electroceramics (F49620-94-1-0428)				5. FUNDING NUMBERS F49620-94-1-0428	
6. AUTHORS Gary L. Messing and Susan Troler-McKinstry					
7. PERFORMING ORGANIZATION NAME(S) AND ADDRESS(ES) Materials Research Laboratory Pennsylvania State University University Park, PA 16802				8. PERFORMING ORGANIZATION REPORT NUMBER	
9. SPONSORING/MONITORING AGENCY NAME(S) AND ADDRESS(ES) Department of the Air Force Air Force Office of Research Attn: Alexander Pechenik Bolling Air Force Base, DC 20332-0001				10. SPONSORING/MONITORING AGENCY REPORT NUMBER	
11. SUPPLEMENTARY NOTES					
12a. DISTRIBUTION/AVAILABILITY STATEMENT  AIR FORCE OFFICE OF SCIENTIFIC RESEARCH (AFOSR) NOTICE OF TRANSMITTAL DTIC. THIS TECHNICAL REPORT HAS BEEN REVIEWED AND IS APPROVED FOR PUBLIC RELEASE LAW AFR 190-12. DISTRIBUTION IS UNLIMITED.					
13. ABSTRACT (Maximum 200 words) <b>Executive Summary</b>  Fiber textured bismuth titanate ( $\text{Bi}_4\text{Ti}_3\text{O}_{12}$ ) (BIT) and biaxially textured La-doped $\text{Sr}_2\text{Nb}_2\text{O}_7$ (SN) were produced by templated grain growth. Platelets of BIT and blade-shaped SN template particles were dispersed in a matrix of nanosize BIT and fine SN powders, respectively, and aligned by tape casting. As determined by x-ray diffraction and microscopy, the sintered ceramics were >90% textured. Growth of the template particles depends critically on the presence of a liquid during growth and maintaining a template to matrix grain size ratio >2.  Textured Nb-doped bismuth titanate ceramics ( $\text{Bi}_4\text{Ti}_{3-x/5}\text{Nb}_{x/5}\text{O}_{12}$ , where $x=0.02$ ) showed anisotropic dielectric and piezoelectric properties when measured parallel and perpendicular to the texture axes with the remanent polarization differing by more than a factor of 15 in the two directions. The piezoelectric constant in the c-axis was ~30 pC/N, or ~77% of the single crystal value. High temperature piezoelectric applications are possible up to ~450°C in textured, doped bismuth titanate.  A gated doctor blade was developed to achieve biaxial alignment of the blade-shaped $\text{Sr}_2\text{Nb}_2\text{O}_7$ template particles. Very good orientation was achieved perpendicular to the major blade axis. In addition, X-ray diffraction measurements of the 131 pole revealed that the $\text{Sr}_2\text{Nb}_2\text{O}_7$ was biaxially textured and had a full width at half maximum of the peak height of 30° in the orientation distribution in the plane of the blades.					
14. SUBJECT TERMS Piezoelectric ceramics, texture, template grain growth, orientation				15. NUMBER OF PAGES 52	
				16. PRICE CODE	
17. SECURITY CLASSIFICATION OF REPORT unclassified	18. SECURITY CLASSIFICATION OF THIS PAGE unclassified	19. SECURITY CLASSIFICATION OF ABSTRACT unclassified	20. LIMITATION OF ABSTRACT		

NSN 7540-01-280-5500

Computer Generated

STANDARD FORM 298 (Rev 2-89)

Prescribed by ANSI Std Z39-18

298-102

DTIC QUALITY INSPECTED 1

20010221140

Department of the Air Force  
Air Force Office of Research  
Attn: Alexander Pechenik  
Bolling Air Force Base, DC  
20332-0001

Final Technical Report for

**TEMPLATED GRAIN GROWTH OF SINGLE CRYSTAL-LIKE  
ELECTROCERAMICS (F49620-94-1-0428)**

Gary L. Messing and Susan Trolier-McKinstry, Principal Investigators

Submitted: January 2001

20010221 140

## Executive Summary

Fiber textured bismuth titanate ( $\text{Bi}_4\text{Ti}_3\text{O}_{12}$ ) (BIT) and biaxially textured La-doped  $\text{Sr}_2\text{Nb}_2\text{O}_7$  (SN) were produced by templated grain growth. Platelets of BIT and blade-shaped SN template particles were dispersed in a matrix of nanosize BIT and fine SN powders, respectively, and aligned by tape casting. As determined by x-ray diffraction and microscopy, the sintered ceramics were >90% textured. Growth of the template particles depends critically on the presence of a liquid during growth and maintaining a template to matrix grain size ratio >2.

Textured Nb-doped bismuth titanate ceramics ( $\text{Bi}_4\text{Ti}_{3-x/5}\text{Nb}_{x/5}\text{O}_{12}$ , where  $x=0.02$ ) showed anisotropic dielectric and piezoelectric properties when measured parallel and perpendicular to the texture axes with the remanent polarization differing by more than a factor of 15 in the two directions. The piezoelectric constant in the  $c$ -axis was  $\sim 30$  pC/N, or  $\sim 77\%$  of the single crystal value. High temperature piezoelectric applications are possible up to  $\sim 450^\circ\text{C}$  in textured, doped bismuth titanate.

A gated doctor blade was developed to achieve biaxial alignment of the blade-shaped  $\text{Sr}_2\text{Nb}_2\text{O}_7$  template particles. Very good orientation was achieved perpendicular to the major blade axis. In addition, X-ray diffraction measurements of the 131 pole revealed that the  $\text{Sr}_2\text{Nb}_2\text{O}_7$  was biaxially textured and had a full width at half maximum of the peak height of  $30^\circ$  in the orientation distribution in the plane of the blades.

## Report Summary

### INTRODUCTION

The electronics industry uses many polycrystalline and single crystal ceramic materials. Most single crystals, like silicon, are grown from the melt by Czochralski and Bridgman techniques. Many multicomponent ceramic materials, however, cannot be produced in this manner as a result of compositional instability at high temperatures or simply because of the high melting temperature and the inevitable problem of contamination. In some cases flux growth techniques, which are based on the use of halides and low melting materials like  $\text{PbO}$ ,  $\text{PbF}_2$ ,  $\text{B}_2\text{O}_3$ , and mixtures thereof, have been developed. However, many of the single crystals produced by these techniques are too costly for widespread application.

Vapor phase techniques are widely used for thin film applications. But, vapor deposition techniques are generally limited to micrometer/hr deposition rates, and thus are too costly for the synthesis of bulk crystals in most cases. The difficulties are exacerbated when the material is multiple element. Also, only single crystal-like ceramics can be produced by vapor techniques. Thus, while a large number of potential applications exist for bulk single crystals, current processes are either not capable of producing the desired material or are prohibitively expensive. Also, the techniques used for the preparation of single crystals require such highly specialized equipment that the synthesis of bulk crystals of many materials cannot be attempted and thus the materials remain unexplored. Many electroceramic materials fall into this latter class of materials.

In this report, we describe a novel Templated Grain Growth (TGG) technique for producing textured materials. Textured means that essentially all of the grains are oriented along at least one axis and thus the properties are intermediate between those of a polycrystalline ceramic and a single crystal. In the extreme case, there would be no grain boundaries and a true single crystal would be produced. TGG processes have a number of attractive features for producing textured materials including (1) solid state reactions can be used to produce precursor materials for TGG that cannot be prepared in bulk form by either vapor or liquid crystal growth techniques, (2) stoichiometry and purity are established during fabrication of the ceramic and retained during TGG, (3) the process is relatively simple and operates at lower temperatures, thus ensuring lower costs, and (4) bulk materials can be fabricated.

Highly textured and single crystal materials have been produced by what we term (1) surface TGG and (2) TGG (Figure 1). In both cases a single crystal is introduced as a

template to initiate directional growth by solid phase epitaxy. For example, a single crystal in contact with a polycrystalline matrix was used to template subsequent grain growth of ferrites to produce single crystals.<sup>1</sup> TGG was initiated<sup>2</sup> by dispersing and orienting single crystals in a sol gel precursor to alumina. Subsequent heating resulted in a highly textured material.

## BACKGROUND ON TEMPLATED GRAIN GROWTH

While there has been little theoretical work on TGG before this study, a few examples from the literature and the PIs' research are described below to demonstrate the potential for such processes and to identify some of the emerging principles.

Case 1 Single crystal ferrites have been produced by a low cost, patented process described by Matsuzawa et al. at NGK Insulators, Inc.<sup>1</sup> for application in video cameras. The process involves placing a fine-grained (5  $\mu\text{m}$ ), dense polycrystalline ferrite in contact with a ferrite single crystal. When heated, the boundary between the single crystal and the polycrystalline matrix grows into the polycrystalline matrix. Although there are no details concerning transport, kinetics and grain boundary mobility, a number of process requirements are identified as important for obtaining single crystals. These include intimate contact at the interface between the two materials, a matrix with a fine grain size, separation of the temperatures for exaggerated grain growth and normal grain growth, and purity.

To achieve an intimate interface, the two materials were polished and a ferrite precursor solution was used to 'activate' growth between the two materials. The patent does not describe the importance or function of this interlayer but simply states that it is necessary. The NGK group also reported the templated grain growth of yttrium iron garnet (YIG)<sup>3</sup> single crystals for magneto-optical applications. Yamamoto and Sakuma<sup>4</sup> reported the application of a similar process for the production of  $\text{BaTiO}_3$  single crystals but again no information concerning the fundamental processes was reported. A recent study on TGG of  $\text{BaTiO}_3$  single crystals reported the properties of BT and Zr-doped BT crystals were comparable to those grown by flux techniques<sup>5-7</sup>.

Case 2 We first reported a process for producing textured alpha alumina by in situ solid phase epitaxy<sup>2</sup>. The process relies on the alignment of acicular (0.1 by 0.5  $\mu\text{m}$ ), single crystal particles of hematite ( $\alpha\text{-Fe}_2\text{O}_3$ ) by drawing fibers from an  $\alpha\text{-Al}_2\text{O}_3$  precursor sol containing the acicular particles. During fiber drawing the acicular particles align in the fiber axis in the  $[10\bar{1}0]$  direction.

From TEM studies we determined that when heated, the  $\alpha\text{-Al}_2\text{O}_3$  epitaxially crystallizes on the acicular  $\alpha\text{-Fe}_2\text{O}_3$  particles with the orientation relationship  $[0001]\alpha\text{-}$

$\text{Al}_2\text{O}_3 \parallel [0001]\alpha\text{-Fe}_2\text{O}_3$  and  $\{11\bar{2}0\}\alpha\text{-Al}_2\text{O}_3 \parallel [11\bar{2}0]\alpha\text{-Fe}_2\text{O}_3$ .<sup>8</sup> At higher temperatures the fibers densify first and then the oriented  $\alpha\text{-Al}_2\text{O}_3$  grains begin to grow into the fine grain alumina matrix. Although not the objective of the study, grains were observed to grow across the entire diameter (20  $\mu\text{m}$ ) of the fibers and to 35  $\mu\text{m}$  in length.

A critical factor for the grain growth of the aligned alumina grains was to achieve a fully dense and ultrafine grain size (<0.5  $\mu\text{m}$ ) matrix prior to the onset of grain growth. In this particular example, low temperature densification and an initially ultrafine grain matrix were obtained by seeding the bulk precursor.

Case 3 A third approach for producing single crystals that is relevant to this proposal is the use of liquid precursors for thin film deposition and crystallization. This is important because such precursors are used later as a means for coupling a single crystal to the polycrystalline matrix. Recently, a number of authors have deposited thin films of precursor solutions onto single crystal substrates. During heating, the nanocrystalline porous film that is formed undergoes densification and epitaxial growth. Single crystal thin films of  $\text{LiNbO}_3$  on sapphire<sup>9</sup>,  $\alpha\text{-Al}_2\text{O}_3$  on  $\alpha\text{-Fe}_2\text{O}_3$ ,<sup>8</sup> YBC on  $\text{SrTiO}_3$ ,<sup>10</sup>  $\text{TiO}_2$  on rutile<sup>11</sup>, and  $\text{ZrO}_2$  ( $\text{Y}_2\text{O}_3$ ) on  $\text{ZrO}_2$  single crystals<sup>12</sup> have been demonstrated. Surprisingly, there have been few studies on how a single crystal film is obtained by this sequence of events. However, this process is similar to Case 2 in that a precursor is heated in contact with a single crystal and thus the grains in direct contact with the substrate become oriented during crystallization.

From the above examples a few common principles important for TGG emerge. These principles can be classified in terms of the interface requirements, matrix requirements for grain growth and process requirements. Critical to the success of the TGG approach is that solid phase epitaxy occurs between the substrate and the fine grain matrix. If the substrate is the same material then there is no lattice parameter mismatch and matrix growth is initiated by homoepitaxy and there are no limitations imposed on grain growth as a result of interfacial strain. In contrast, when a crystallographically similar material is used, then the lattice parameter mismatch is accommodated by the formation of misfit dislocations and lattice strain. If the mismatch is too large the residual strain energy may offset the driving force for grain growth in a thin film<sup>12</sup>. In this case no grain growth would be expected, as there is no thermodynamic driving force for boundary motion. Based on these limited studies, one would conclude that homoepitaxy is the preferred approach so that all of the grain boundary energy is available to drive grain growth. However, single crystals or appropriately shaped template particles of some materials are simply not available.

The grain size of the matrix relative to the template dimension is clearly one of the most important criteria for TGG because the driving force for boundary migration is the grain boundary free energy. As grains begin to decrease to  $<0.5\text{ }\mu\text{m}$ , the growth of matrix grains can occur at a much lower temperature and thus temperature regimes where the material is prone to exaggerated grain growth can be avoided.

## RESEARCH OBJECTIVE

The goal of the program was to determine to what extent single crystal or single crystal-like, textured materials could be produced by templating solid state grain growth and to develop a scientific understanding of the TGG process. We studied TGG of  $\text{Bi}_4\text{Ti}_3\text{O}_{12}$  and  $\text{Sr}_2\text{Nb}_2\text{O}_7$  because of the strongly anisotropic properties of these materials and the high potential impact of such materials as high temperature piezoelectrics. Also, because  $\text{Sr}_2\text{Nb}_2\text{O}_7$  and  $\text{Bi}_4\text{Ti}_3\text{O}_{12}$  are members of the layered perovskite and bismuth oxide layer structure crystal families, respectively, the results of this study would give insights about how to produce textured electroceramics in these two crystal families.

To achieve the research goals we undertook the following tasks

- Study the TGG of  $\text{Sr}_2\text{Nb}_2\text{O}_7$  and  $\text{Bi}_4\text{Ti}_3\text{O}_{12}$
- Characterize microstructure texture, interfaces and defects to determine what phenomena control template growth.
- Determine the electrical and electromechanical properties of the textured materials as a function of the process parameters and degree of texture.
- To provide fundamental information about growth as a function of specific crystallographic direction. This topic was supported via an AASERT and the results were reported separately.<sup>5-7</sup>

## Materials

High temperature piezoelectrics are very attractive for remote sensing in hostile environments. For example, in order to improve fuel efficiency, as well as the ignition timing in automobile engines, acoustic sensors, which detect the onset of engine knock, are used. However, currently available materials such as lead zirconate titanate cannot be mounted too close to the engine, as the ambient temperature is high enough to either depole the ceramic or in some cases to raise it through the Curie temperature. Consequently, for such applications, there is a need to develop materials that remain piezoelectric at high temperatures. In addition to acceptable piezoelectric properties, a high electrical resistivity at elevated temperatures is required.  $\text{Sr}_2\text{Nb}_2\text{O}_7$  is an excellent candidate for these applications as it has one of the highest Curie temperatures of known ferroelectrics. Similarly,

$\text{Bi}_4\text{Ti}_3\text{O}_{12}$ , with a Curie temperature of  $675^\circ\text{C}$  is already in limited use as a high temperature piezoelectric<sup>13</sup>.

### **Bismuth Titanate ( $\text{Bi}_4\text{Ti}_3\text{O}_{12}$ )**

In the present work, TGG was applied to the ferroelectric ceramic  $\text{Bi}_4\text{Ti}_3\text{O}_{12}$ . BiT is an excellent material for the study of this process for several reasons. It is a candidate for use in high temperature piezoelectric devices because of its high Curie temperature ( $675^\circ\text{C}$ ). However, poling the ceramic is difficult because low crystal symmetry inhibits the appropriate orientation of the polarization axes, which lie in the *a-c* plane of the monoclinic crystals<sup>14</sup>. Texture increases poling efficiency by aligning crystallographic axes, enhancing the piezoelectric properties.

It has been shown that plate-like particles of BiT, made by molten salt synthesis, can be oriented by hot forging<sup>15,16</sup> and by tape casting<sup>17</sup>. The platelets are apparently single crystals (monoclinic at room temperature) with the *c*-axis perpendicular to the major faces. Appropriate processing orients the crystals along the *c*-axis, face to face. Tape casting has the advantage of lower cost relative to forging or hot pressing.

Anisotropy in the low field dielectric properties has been previously reported for TGG bismuth titanate (BiT) ceramics.<sup>18,19</sup> However, due to the high electrical conductivity in the *a-b* plane, where the major component of the polarization lies, poling was difficult. This complicates examination of ferroelectricity and piezoelectricity in undoped grain-oriented bismuth titanate. Recently, it was shown that donor-doping bismuth titanate with group V (Nb, Ta, Sb) and group VI (W) elements reduces the electrical conductivity by 3-4 orders of magnitude up to  $\sim 600^\circ\text{C}$  and facilitates both poling and the use of bismuth titanate at elevated temperatures.<sup>20</sup>

The objectives of this study were to develop a TGG approach to produce textured BIT and textured Nb-doped bismuth titanate ceramics and to measure the dielectric and piezoelectric properties of the resulting materials.

### **EXPERIMENTAL PROCEDURES**

A coprecipitation method was developed for making ultrafine  $\text{Bi}_4\text{Ti}_3\text{O}_{12}$  particles. Powder calcined at  $700^\circ\text{C}$  was comprised of equiaxed particles, having an average diameter of about 200 nm and specific surface area of  $8\text{ m}^2\text{g}^{-1}$  which corresponds to an equivalent spherical diameter of 93 nm, indicating that the particles are aggregates of a few primary particles.

Platelike particles were prepared by mixing equal weights of the dry amorphous powder and a eutectic mixture of NaCl and KCl in a sealed crucible and heating to  $1100^\circ\text{C}$ ,



above the melting point of the salt. The mixture was heated at a rate of 10°C/min, and held at temperature for 12 minutes before slowly cooling. It was then washed with warm deionized water to remove the alkali metals and chlorine, and dried under vacuum. The platelets were approximately 5 - 20  $\mu\text{m}$  in diameter and 0.5  $\mu\text{m}$  thick (Figure 2).

Slurries for tape casting were prepared with 15 vol% powder in a commercial organic binder solution (B73305, FERRO). Calcined BiT powder was dispersed in toluene with a polymeric dispersant (KD3, ICI Specialty Chemicals) using an ultrasonic horn. The dispersion was added to the binder solution in a Nalgene bottle containing a small amount of  $\text{ZrO}_2$  media and mixed on a roller mill for 24 h. The slurry was then poured into a beaker and covered. BiT platelets (5 or 10 % of the fine powder volume) were dispersed in toluene with KD3 using an ultrasonic bath, then stirred into the powder-binder mixture with a magnetic bar. The slurry was stirred until 15 vol% solids was obtained by solvent evaporation (determined gravimetrically).

Tapes were cast at 7.5 cm/s with a blade opening of 200  $\mu\text{m}$  on a glass surface and dried under ambient conditions, producing 60  $\mu\text{m}$  thick tape. The tapes were cut into pieces approximately 5  $\text{cm}^2$ , stacked in layers of 10, heated to 70°C and pressed uniaxially at 50 MPa.

Densities of the sintered samples were measured by the Archimedes method. Texture was calculated from x-ray diffraction data by the Lotgering method. Samples were scanned from  $2\theta = 10^\circ$  to  $80^\circ$  on the surface parallel to the casting plane. The degree of orientation,  $f$ , is defined as  $f = (p - p_0)/(1 - p_0)$ , where  $p = \Sigma I_{\{00\ell\}}/\Sigma I_{\{hkl\}}$  for intensities,  $I$ , between  $2\theta = 10^\circ$  and  $80^\circ$ . The calcined powder was used as a randomly oriented standard to determine  $p_0$ .

Nb-doped bismuth titanate precursors were synthesized by coprecipitation of  $\text{Bi}_2\text{O}_3$  and  $\text{TiO}(\text{OH})\text{Cl}$  in a nitric acid solution by the dropwise addition of  $\text{NH}_4\text{OH}$ . Niobium in the form of Nb-oxalate (Niobium Products, Pittsburgh, PA) was substituted for Ti before coprecipitation. The chemical formula was  $\text{Bi}_4\text{Ti}_{3-x/5}\text{Nb}_{x/5}\text{O}_{12}$ , where  $x=0.2$ . The as-dried powder was calcined at 700°C for 0.5h. Bismuth titanate template particles were synthesized by heating a mixture of as-dried bismuth titanate powder with NaCl and KCl at 1100°C for 12 min. The salts were removed by washing the platelets with distilled water more than five times. This produced large tabular particles with the major face perpendicular to the crystallographic  $c$ -axis.

Tape casting slurries of Nb-doped bismuth titanate ( $x=0.2$ ) were prepared by mixing 30 vol% powder with a commercial non-aqueous binder solution (B73305, Ferro Corp., San Marco, CA). The slurries were cast onto a glass plate with a doctor-blade at a blade height of 300  $\mu\text{m}$  and at a casting speed of 7 cm/sec. The template concentration was

5 wt% of the BiT. The tapes were cut, laminated, pressed uniaxially at 40 MPa, and calcined at 450°C for 2 h. Additional processing details about the powder and template particles were described earlier.<sup>19,21</sup>

Pressing the calcined powder produced randomly oriented samples. Samples were sintered between 950 and 1100°C for 2h. Phase analysis and grain orientation of sintered samples was examined by XRD. The apparent density was measured by the Archimedes method and microstructures were observed by SEM. The dielectric constants of polished, Pt electroded samples were measured between 30 and 450°C at 10 and 100 kHz. The remanent polarization and coercive field were obtained at room temperature using a modified Sawyer-Tower circuit. Nb-doped samples were poled for 10 sec to 20 min in a silicone oil bath at 200°C at an electric field of 40-90 kV/cm. Due to the lower resistivity of undoped BiT samples they were poled at 20 kV at 150°C for 5 min. The piezoelectric constants of poled samples were measured using a Berlincourt  $d_{33}$  meter at a frequency of 100 Hz. The dielectric properties were measured both parallel and perpendicular to the casting plane of the textured samples. Thermal depoling experiments were conducted by holding the poled samples for 10 min at each temperature, cooling to room temperature, measuring  $d_{33}$ , and repeating the procedures at intervals of 50°C up to 700°C.

## RESULTS

The sintered densities of both templated and untemplated laminates are shown in Figure 3. The dilatometry data indicated a sharp maximum in the densification rate near 870°C. From a green density of 48% the maximum sintered density of 97% was obtained at 1000°C in less than 10 minutes. The attainment of high density at relatively low sintering temperatures is believed to result from the fine grain size of the matrix material. The presence of template particles did not affect sintered densities at  $\geq 950^\circ\text{C}$ . Shrinkage was anisotropic; 25-30% in thickness and 10-15% along either side.

In the laminates containing no template particles, grains are on the order of 1 micron and mostly anisometric after heating for 10 minutes at 1000°C. Longer sintering times result in the growth of large anisometric grains, some  $>10\ \mu\text{m}$  after 2 hours. At 1100°C, many anisometric grains  $\approx 2\text{-}10\ \mu\text{m}$  in diameter are present after 10 minutes.

Figure 4 shows the as-sintered edge of a templated laminate, sintered at 900°C for 10 minutes. The matrix is  $\approx 90\%$  dense and no appreciable grain growth is apparent. After 2 hours at 900°C, the matrix remains fine-grained. Reasonable orientation of the template particles is apparent.

For short sintering times at 1000°C and higher (Fig. 5), laminates containing 5% template particles develop oriented grains. The microstructures consist primarily of plate-

like grains, approximately 10-50  $\mu\text{m}$  long and 1-2  $\mu\text{m}$  thick, aligned in the casting plane. Little change in the average grain size or orientation was observed between 10 minutes and 2 hours at 1000°C. Figures 5a and 5b show that grains misaligned with the casting plane do not grow as large as the oriented grains.

Sintering at 1100°C for less than 10 minutes produced microstructures similar to those at 1000°C. After one hour, however, grain thickness increased by approximately 1.5 times, and a second phase appeared. XRD peaks indicative of the cubic phase  $\text{Bi}_2\text{Ti}_2\text{O}_7$  suggest that bismuth volatilization at the grain surfaces caused the formation of the bismuth deficient phase. Observations of weight loss during sintering (approximately 1 wt% per hour above 1050°C) support this interpretation.

X-ray diffraction data reveal the effect of template particles on texture development. With increased sintering temperature, diffraction from the  $\{00\ell\}$  planes progressively dominates the pattern. The degree of orientation (Lotgering factor,  $f$ ) is shown in Figure 6 as a function of sintering temperature. For untemplated laminates, this factor remained below 0.25 irrespective of the sintering temperature. Texture in the templated samples was observed to increase strongly with the sintering temperature, approaching 0.96 above 1000°C for samples containing either 5% or 10% template particles. This degree of orientation is as high as that reported for samples tape cast and sintered with 100% platelets<sup>17</sup>. Texture developed very rapidly at temperature, as shown in Figure 7 for sintering at 1050°C.

The effect of lamination pressure on platelet orientation was observed in a series of samples pressed at different loads and sintered for 1 h at 1050°C. No systematic change in the Lotgering factor,  $f$ , was observed for pressures up to 120 MPa. Furthermore, the average value of  $f$  for laminated samples did not significantly increase relative to single tape samples. This indicates that orientation of the template particles was achieved by tape casting alone and that lamination did not enhance template alignment. Delamination was observed after sintering in samples pressed at less than 30 MPa, so 50 MPa was used as the standard pressure.

To determine the variation in texture through the sample thickness, two laminates of ten tapes (each approximately 300  $\mu\text{m}$  thick) with 5% templates, sintered at 1050°C for 1 hour, were successively ground and tested by XRD. There was no systematic decrease in preferred orientation with distance from the surface, remaining greater than  $f = 0.90$  for one sample and greater than  $f = 0.94$  for the other. Since the higher texture corresponds to a lower lamination pressure, the differences are considered a result of sample to sample variations rather than effects of pressure. This texture profile is contrasted with that of the

tape cast and sintered platelets of Watanabe *et al.*<sup>17</sup>, which showed a degree of texture less than 0.7 in the interior of the laminates. The reason for improved through-thickness texture by TGG processing is most likely the small interparticle spacings achieved by using fine powder. Frequent interparticle interaction during tape casting is expected to enhance the alignment of platelets. The orientation of platelets during tape casting is critical for obtaining high quality texture and is discussed elsewhere<sup>21</sup>.

The as-dried Nb-doped bismuth titanate precursor powder was amorphous, but transformed to crystalline bismuth titanate after calcination at 700°C for 0.5 h. There were no shifts in the BiT x-ray diffraction pattern with Nb-doping (up to  $x=0.4$ ) for either calcined powders or sintered samples<sup>22</sup>. Nb-doping did not affect the morphology or size of the bismuth titanate powders and platelets during synthesis.

The sintered densities of Nb-doped random and Nb-doped textured samples are shown in Figure 8. Low temperature densification was promoted by the fine particle size of the precursor powder. The relative density reached a maximum of 98-99% (based on a theoretical X-ray density of 8.04 g/cm<sup>3</sup>) at 1000°C for 2h, which is higher than reported in previous studies for similar sintering conditions.<sup>22</sup> Above 1100°C, the density decreased as a result of the extensive growth of the tabular bismuth titanate grains. Samples containing template particles densified at ~50-100°C lower than compacts composed of only BiT platelets.

The SEM micrographs of the randomly oriented samples exhibit mixed grain microstructures of equiaxed and platelike grains at 1000°C for both undoped (Fig 9a) and Nb-doped Fig 9b) samples. Grain growth of BiT was enhanced with Nb-doping level ( $x=0.2$ ) but it was inhibited at  $x=0.4$ . Consequently, only results for the  $x=0.2$  Nb are presented.

Microstructures of textured Nb-doped BiT ( $x=0.2$ ), which contained 5 wt% template particles, are shown in Figure 10. The cross-sectional view demonstrates that the bismuth titanate platelet grains are aligned in the casting direction and the top view indicates that the original platelets grew at the expense of fine matrix grains. XRD patterns of textured samples parallel and perpendicular to the casting plane further confirm that textured samples are *c*-axis oriented (Figure 11). The degree of orientation (Lotgering factor, *f*) in samples processed using similar conditions was >0.96.

### Dielectric Properties of Textured Bismuth Titanate

The temperature dependence of the dielectric constant, *K*, and loss tangent,  $\tan \delta$ , of doped random and textured BiT was measured at 100 kHz (Fig. 12). The dielectric properties at 10 kHz are similar to those at 100 kHz. Pure, randomly oriented bismuth

titanate ceramics (sintered at 1050°C for 2h) exhibit a room temperature dielectric constant of ~145, and Nb-doping slightly increases the room temperature dielectric constant for the same conditions. With increasing sintering temperature, the room temperature dielectric constant decreases for all random samples, which is probably due to the density decrease. The dielectric constant and loss tangent in undoped samples rapidly increase above 200°C because of the high electrical conductivity. However, Nb-doping clearly reduced the dielectric loss; the loss tangent is below 0.1 up to 450°C, which enables poling at higher electric fields and higher temperatures. The textured ceramics show anisotropic dielectric constants of ~160 parallel to and ~120 perpendicular to the casting plane. These values are smaller than single crystal room temperature values ( $K_a=120$ ,  $K_b=205$ ,  $K_c=140$  at 5 MHz).<sup>13</sup> The higher dielectric loss in the tapes parallel to the casting direction is due to the higher conductivity in the *a-b* plane of bismuth titanate.<sup>14</sup>

The room temperature polarization-electric field hysteresis loops of random and textured samples that have been sintered at 1050°C for 2h are shown in Fig. 13. The remanent polarization for the Nb-doped random BiT is ~12  $\mu\text{C}/\text{cm}^2$ . The loops for the doped samples are better saturated and have a smaller coercive field than those for undoped random BiT. The reduction in coercive field is probably a result of the larger grain size in the doped samples. Anisotropic remanent polarizations ( $P_r$ ) and coercive fields ( $E_c$ ) are observed in the sintered tapes:  $P_r=24.5 \mu\text{C}/\text{cm}^2$ ,  $E_c=30 \text{ kV}/\text{cm}$  parallel to and  $P_r=1.4 \mu\text{C}/\text{cm}^2$ ,  $E_c=10 \text{ kV}/\text{cm}$  perpendicular to the casting plane. These values are close to those previously reported for hot-forged bismuth titanate.<sup>16</sup> In bismuth titanate, the spontaneous polarization  $P_s$  lies in the monoclinic *a-c* plane at a small angle (~4.5°) to the *a*-axis and exhibits two independently reversible components: 50  $\mu\text{C}/\text{cm}^2$  along the *a*-axis and 4  $\mu\text{C}/\text{cm}^2$  along the *c*-axis.<sup>14</sup> The observed remanent polarization of the textured sample is about half of the spontaneous polarization of single crystal bismuth titanate in either direction.

The variations of piezoelectric constant of doped BiT with respect to poling time and applied electric field are shown in Fig. 14. The piezoelectric constant increases monotonically with applied field up to 80 kV/cm and is saturated within 10 min. The measured piezoelectric constants of the random and textured ceramics are shown in Fig. 15. Random Nb-doped samples show  $d_{33}$  values of ~20 pC/N, which are comparable to earlier reports.<sup>24</sup> Due to the improved orientation, the textured samples exhibited anisotropic piezoelectric behavior with a maximum piezoelectric constant of ~30 pC/N parallel to the casting plane. The reported piezoelectric constants for a single domain single crystal are:  $d_{11} = 39 \text{ pC}/\text{N}$ ,  $d_{22} = 0$ , and  $d_{33} = 9 \text{ pC}/\text{N}$ .<sup>25</sup> Thus, the maximum piezoelectric constant of the

textured sample is about 77% of the single crystal value measured along the major polarization axis. Grain orientation in the *a*- and *b*-axes is random in the casting plane so it is reasonable that the measured values fall below the single crystal numbers.

Thermal depoling of samples is shown in Fig. 15, in which piezoelectric constants are plotted against annealing temperature. Both Nb-doped random samples and textured samples retain 90% of their room temperature values up to 600°C for a 10 minutes exposure to the annealing temperature when annealed under open circuit conditions. Also the Nb-doped sample retained more than 90% of its initial value after annealing for 100 h at 450°C. This demonstrates that the Nb-doped, textured bismuth titanate ceramics are stable against thermal exposure, and can potentially be used in high temperature piezoelectric applications.

### **Biaxially Textured Strontium Niobate ( $\text{Sr}_2\text{Nb}_2\text{O}_7$ )**

Textured ceramics have been produced by a variety of techniques. In most cases the texture corresponds to crystallographic orientation along one axis only, which is often referred to as fiber texture. Polycrystalline bodies in which most grains are oriented with a particular crystallographic plane parallel to a common plane in the sample, and with the same crystallographic direction in that plane parallel to a common direction in the sample, exhibit sheet or biaxial texture.<sup>26,27</sup> Such materials exhibit approximately the same property anisotropy as a single crystal of the same composition. The ability to synthesize  $\text{Sr}_2\text{Nb}_2\text{O}_7$  particles in the form of orthorhombic blades<sup>18</sup> makes it possible to develop a ceramic with biaxial texture by TGG.

We describe a gated doctor blade that was designed to facilitate template orientation during tape casting to produce biaxially textured  $\text{Sr}_2\text{Nb}_2\text{O}_7$  ceramics by TGG. Previous studies have shown that template growth during TGG is enhanced with a liquid phase former<sup>18</sup>. In  $\text{Sr}_2\text{Nb}_2\text{O}_7$  it is known that excess Nb induces liquid phase formation but too much liquid (formed by 5 mol% excess niobium) leads to uncontrolled matrix growth whereas small amounts lead to anisotropic grain growth<sup>20,28</sup>. In this paper, the lower limits for the amount of liquid required for TGG in  $\text{Sr}_2\text{Nb}_2\text{O}_7$  were established by studying the effect of small variations in the Nb/Sr ratio on template growth<sup>29</sup>. Texture evolution, as monitored by stereology, x-ray pole figures and dielectric measurements, was studied as a function of template growth kinetics and orientation.

### **Experimental Procedures**

Coprecipitated 2 mol% La-doped  $\text{Sr}_2\text{Nb}_2\text{O}_7$  powder with an average particle size of 0.5  $\mu\text{m}$  was used as the matrix powder for TGG<sup>18</sup>.  $\text{Sr}_2\text{Nb}_2\text{O}_7$  template particles of 20-50

$\mu\text{m} \times 3\text{-}5 \mu\text{m} \times 0.2\text{-}0.5 \mu\text{m}$  ( $a \times c \times b$ ) size were synthesized in KCl using  $\text{SrCO}_3$  and large  $\text{SrNb}_2\text{O}_6$  crystals as the niobium source.<sup>30</sup> The matrix powder was dispersed in 2-propanol by milling for 12 h with a commercial dispersant (KD-2)\*. The binder plus plasticizer system (Ferro B7407)\*\* was added to the suspension, and the slurry was milled for 6 h. The template particles were separately dispersed in 2-propanol with mild ultrasonication for 3 minutes, followed by stirring for 1 h.

The suspension of template particles was slowly added to the matrix powder slurry while stirring. The slurry was stirred for up to 6 h and the solids loading was adjusted to 30-35 vol% by evaporation at room temperature. The slurry was cast at 7-9 cm/s under a gated doctor blade (Figure 17). The blade opening was 300-500  $\mu\text{m}$  and the gates were formed by spacing needles of 0.5 mm diameter 1 mm apart. The gates modify the local shear field under the doctor blade such that the length of the templates orients along the casting direction. The dried tape was stacked (200-500 layers) and laminated at 33 kPa and room temperature for 5 minutes. The binder was removed by heating at 2°C/min to 250°C and holding for 1 h, heating at 2°C/min to 350°C and holding for 1 h, and heating at 3°C/min to 600°C and holding for 1 h.

The amount of liquid formed during TGG was adjusted by varying the Nb to (Sr+La) molar ratio. Stoichiometric Nb/(Sr+La)=1 coprecipitated powder was used in all cases. Excess niobium was added in the form of niobium oxalate to cast samples after binder burnout to prevent binder-oxalate ion interactions, which cause coagulation of the binder. The laminate was impregnated with solutions of niobium oxalate of different concentrations to obtain ppm level compositional variations in the Nb/(Sr+La) molar ratio. The laminates were then heated at 3°C/min to 500°C to convert the niobium oxalate to x-ray amorphous niobium oxide.

Stereological analysis was carried out on three orthogonal planes normal to the  $a$ ,  $b$ , and  $c$  crystallographic directions using NIH image analysis software.<sup>31</sup> The  $b$ -axis was normal to the casting plane, and the  $c$ -plane was normal to the casting direction. The shape of the grown templates can be approximated to a thin, rectangular plate. This implies that grain dimensions of templates obtained from 2-D sections parallel to the casting plane closely approximate the true dimensions along the  $a$  and  $c$ -directions.

Pole figure measurement is a diffraction technique that can be used to collect orientation distribution information from a large number of crystallites. The pole figure for a single crystal resembles the stereographic projection for the set of  $hkl$  planes of interest.

---

\* ICI Chemicals, Wilmington, DE 19850

\*\* Ferro Corp., San Marcos, CA 92062

In the stereographic projections for a single crystal of  $\text{Sr}_2\text{Nb}_2\text{O}_7$ , the 131 family of poles lie at four distinct orientations for projections along the principal crystallographic axes. The 131 plane is also at an angle to the  $a$ ,  $b$ , and  $c$ -planes. Thus, a sample with no texture (i.e., randomly oriented) should produce the same 131-pole density at all orientations. In contrast, a sample with fiber texture should show a ring-shaped region of high intensity for the 131 pole when measured along the alignment direction. The ring is a result of in-plane randomness. However, a sample with biaxial texture should exhibit four distinct peaks at the predicted orientations for the 131 poles in the stereographic projection. Hence, a single 131-pole figure measurement can be used to determine the quality of biaxial texture at room temperature in  $\text{Sr}_2\text{Nb}_2\text{O}_7$ .

A Philips four-circle diffractometer was used to collect pole figure data. The source and detector were fixed in relative  $2\theta$  for the desired reflection throughout the measurement.  $\phi$  was measured from the vertical about an axis along the incident beam from  $0^\circ$  to  $90^\circ$  in increments of  $3^\circ$ . For each value of  $\phi$ , the sample face was rotated one complete rotation in plane in increments of  $10^\circ$  ( $\Omega$  scan). The collection time was set at 5 s at each orientation. Samples of circular geometry ( $\sim 1 \text{ cm}^2$  area) were used to avoid anisotropy artifacts in the  $\Omega$  scan due to different areas of illumination as a result of beam defocusing at high values of  $\phi$ . The pole figure data from a random sample was used to normalize the data collected from textured samples for defocusing and beam spreading as a function of  $\phi$  by subtracting the pole figure of the random sample from that of the textured samples. The randomly oriented sample was made by cold isostatic pressing a pellet of  $(\text{Sr},\text{La})_2\text{Nb}_2\text{O}_7$  at 275 MPa.

The dielectric properties of TGG samples possessing biaxial texture were also measured. Parallel sample surfaces were polished using a final grit of  $1 \mu\text{m}$  diamond paste. Samples were cleaned with water and acetone, and dried. Sputtered platinum was used for electrodes. The capacitance and loss were measured from  $-175^\circ\text{C}$  to  $440^\circ\text{C}$  using an HP4192A LCR bridge and an Euro 808 oven. A 1V signal was used to measure the dielectric properties of samples at 10 KHz, 100 KHz, and 1 MHz.

#### Template Morphology and Biaxial Texture

As seen in Figure 18, the template particles have a long rectangular face and a thickness that is much less than the breadth of the particles. Hartman and Perdok<sup>32</sup> proposed that crystal growth occurs preferentially in directions along uninterrupted series of strong bonds. The directions in which one finds continuous, rigid bonding in  $\text{Sr}_2\text{Nb}_2\text{O}_7$  are coincident with the crystallographic  $a$  and  $c$ -axes. The Nb-O bonds along the  $b$ -axis are discontinuous. Hence, the slowest growth is expected in the  $b$ -direction. X-ray diffraction of



the blade-like particles of  $\text{Sr}_2\text{Nb}_2\text{O}_7$  confirms that the thinnest dimension is parallel to the  $b$ -axis. This is further corroborated by the increase in the intensity of the (0k0) of the grain-oriented samples formed by tape casting.<sup>31</sup> The length of the blade-like particles is parallel to the  $a$ -axis and the width of the face is parallel to the  $c$ -axis.

One way to produce a high, local shear field in the casting plane is to provide a set of closely spaced narrow openings with evenly spaced rods or needles along the length of the doctor blade (Figure 17). For needles of 0.5 mm diameter, which were spaced 1.0 mm apart, an average shear rate of  $\sim 50$  to  $75 \text{ s}^{-1}$  is developed during casting. The relatively high viscosity immediately after the doctor blade allows just enough flow for leveling of the tape due to the surface tension of the cast surface. The specific conditions were a casting shear rate of  $150 \text{ s}^{-1}$ , a viscosity of  $20 \text{ mPas}^{-1}$  under the doctor blade, a blade gap of  $300 \mu\text{m}$ , and a template particle size of  $20 \mu\text{m}$  with an aspect ratio of 5-10 (length to width). Assuming the template aspect ratio, slurry rheology, and spacing between the needles, Peclet numbers of  $1.6 \times 10^{10}$ - $7.4 \times 10^{10}$  were calculated for the flow under the doctor blade in the horizontal plane. The gravitational force on rotating particles during casting and uniaxial lamination also influences the orientation of the  $b$ -planes of the templates parallel to the casting plane.

#### Effect of Excess Niobium on Grain Growth in $(\text{Sr}_{0.99}\text{La}_{0.01})_2\text{Nb}_2\text{O}_7$

TGG samples with 10 vol% initial templates and a small excess of niobium (5-1000 molar ppm) were sintered at  $1350^\circ\text{C}$  and  $1450^\circ\text{C}$ . The  $a$ -direction edges of samples sintered at  $1450^\circ\text{C}$  for 1 h with different amounts of excess niobium are shown in Figure 19. The average area of the template grains increases with increasing niobium concentration. This is contrary to the expectation that a smaller amount of liquid phase results in thinner liquid layers and higher growth rates. One possible reason for this anomaly might be that liquid formation is a result of a reaction, and at such low amounts of excess niobium, the liquid distribution might not result in a continuous film. Bae and Baik<sup>34</sup> observed a similar increase in the growth of alumina grains in the presence of ppm-levels of impurities. Alternatively, the higher Nb content samples may have densified earlier. Thus, with less porosity to pin the crystal-matrix boundary the template grains can grow for a longer time. The larger grains result in a larger area fraction of large anisotropic grains as shown in Figure 20.

To detect whether exaggerated grain growth in the matrix leads to large anisotropic grains, the number density of large ( $>15 \mu\text{m}$ ) anisotropic grains was tracked at  $1350^\circ\text{C}$  and  $1450^\circ\text{C}$  with increasing niobium concentration. The number density of large grains was nearly constant, which indicates that exaggerated grain growth does not contribute to the

population of large grains. These measurements are in agreement with SEM observations, which show very few grains that are not aligned in the expected direction.

The average grain dimensions (major and minor axis of inscribed ellipses) obtained in microstructures sintered at 1350°C and 1450°C for 1 h with different amounts of excess niobium were measured by stereology. The average length in the *a*-axis direction reaches a maximum of ~55 μm for 1200 ppm niobium at 1450°C. In contrast, growth in the *c*-axis direction is only ~7 μm for all Nb concentrations and temperatures studied. The aspect ratios show a slight increase with increasing excess niobium but levels off at ~6. On the basis of these observations, 500-1000 ppm of excess niobium was used to fabricate TGG samples.

#### Grain Growth Kinetics of Biaxially Textured $(\text{Sr}_{0.99}\text{La}_{0.01})_2\text{Nb}_2\text{O}_7$ Ceramics

Grain growth was studied as a function of time at 1450°C in samples containing 1000 ppm excess niobium and 10 vol% initial templates. Microstructures of sample sections parallel to the *c*-plane and sections parallel to the *b*-plane sintered at 1450°C for 1, 10, 30, and 60 minutes were analyzed. Microstructures after 1 and 60 min at 1450° are shown in Figure 21. The difference in the dimensions of the blade-shaped grains implies that they are biaxially oriented.

Figure 22 shows the 131 pole figure data for samples sintered at 1500°C for 4 h. The four distinct peaks at positions coinciding with the calculated 131 poles in the stereographic projection conclusively prove the presence of biaxial texture in  $(\text{Sr},\text{La})_2\text{Nb}_2\text{O}_7$  TGG samples with the *b*-axis perpendicular to the tape cast plane and the *a*-axis parallel to the tape casting direction of the sample. The FWHM is ~30° in the arc joining the maxima of the 4 peaks as compared to 90° for a random sample.

The x-ray diffraction patterns from the planes parallel to *a*, *b*, and *c*-crystallographic planes of samples sintered at 1500°C for 4 h are shown in Figure 23. The enhancement of the 200, 080, and 002 peaks, respectively, further supports the claim that these samples are biaxially textured.

The size of the template grains along the *a*, *b*, and *c*-directions was determined from stereological measurements. Only grains with major axes longer than 15 μm were included in the calculation of the template size and orientation statistics because the average matrix grain size was 5-10 μm. The major and minor axes of an inscribed ellipse, grain area, the angle between the major axis and the *b*-direction in the *c*-plane, and the angle between the major axis and the *c*-direction in the *b*-plane were measured using the NIH image software. Figure 24 shows the angular distribution of template orientations measured at 5° intervals. For a template particle that has attained the ideal orientation, the angle is 90° for both the *b*

and *c*-planes. Figure 24 shows the orientation distributions after 1 min and 60 min for the grain number percent. The distributions become sharper at  $\sim 90^\circ$  because of the growth of the template particles. This suggests that there is no reorientation or rotation of template particles. Another feature of these distributions is the sharp peak around  $90^\circ$  in the two planes of projection perpendicular to each other. In the third plane, the *a*-plane, it is difficult to distinguish the template grains from the matrix grains because they have similar cross sections. However, at conditions that lead to high degrees of textured material, such as  $1500^\circ\text{C}$ , 4 h, the angular distribution of oriented grains in the *a*-plane revealed a similar distribution centered on  $90^\circ$  with respect to the *b*-direction. This indicates that the particles are oriented in all three directions, and thus, actions parallel to their *a*, *b* and *c*-planes yield the true dimensions of the *a*, *b*, and *c* -grains.

Growth in the *a*- and *b*-directions is seen to reach a maximum after 30 min. Again, the number density of large templates does not change significantly, which means that the template grains dominate the grain growth process. The biaxial texture is shown in Figure 25 for a sample sintered at  $1450^\circ\text{C}$  for 1 h.

Figure 26 shows the dielectric behavior of biaxially textured TGG samples of  $(\text{Sr},\text{La})_2\text{Nb}_2\text{O}_7$  sintered at  $1500^\circ\text{C}$  for 4 h. The room temperature dielectric constants in the *a*, *b*, and *c* directions were 68, 45, and 49, respectively. These values are similar to those of single crystal  $\text{Sr}_2\text{Nb}_2\text{O}_7$  ( $K_a=73$ ;  $K_b=46$ ;  $K_c=43$  at  $25^\circ\text{C}$  measured at 1 MHz). While some of the anisotropy may be due to different numbers of grain boundaries in the three perpendicular cuts, the difference in the temperature coefficients for the permittivity demonstrates that at least some of the observed anisotropy is due to the sample texture. In particular,  $K_b$  remains lower than  $K_c$  at  $> 25^\circ\text{C}$ , and starts to rise as the temperature approaches  $-156^\circ\text{C}$ . The dielectric constant in the *b*-direction for single crystals shows similar behavior with a peak at  $-156^\circ\text{C}$  due to the phase transition that results in a small component of  $P_s$  along the *b*-direction. This rise is not as marked in the *a* and *c*-direction dielectric constants for the biaxially-textured TGG samples. The dielectric loss is plotted as a function of temperature in Figure 26.

## CONCLUSIONS

$\text{Bi}_4\text{Ti}_3\text{O}_{12}$  was synthesized as fine powder and as large platelets for use in Templated Grain Growth studies. High densities (97%) were obtained in tape cast, laminated and sintered samples at temperatures as low as  $1000^\circ\text{C}$ . Texture in the ceramic, characterized by a Lotgering factor of approximately 0.96, was induced by TGG after alignment of the large particles by tape casting. The temperature at which ultimate density was attained, and the

constant through-thickness texture profile are unprecedented for tape cast and conventionally sintered BiT.

Templated grain growth of Nb-doped bismuth titanate ceramics produced well-oriented materials with high electrical resistivity. Dense and textured microstructures (>98%) were obtained by sintering a fine-grained matrix at temperatures as low as 1000°C. The oriented ceramics exhibited anisotropic dielectric and piezoelectric properties parallel and perpendicular to the casting plane. The maximum piezoelectric constant in the c-axis was 77% of the single crystal value. Sintered samples retain >90% of the room temperature piezoelectric constant up to 600°C for 10 min or at 450°C for 100 h. While the dielectric and piezoelectric properties are comparable to those of hot-forged bismuth titanate ceramics, the relative ease of the TGG process may enable commercial access to textured ceramics because of the significantly lower processing costs of TGG.

Biaxial texture can be induced by templated grain growth in  $\text{Sr}_2\text{Nb}_2\text{O}_7$  ceramics. Blade-like  $\text{Sr}_2\text{Nb}_2\text{O}_7$  templates can be oriented to achieve biaxial texture by gated tape casting. The amount of excess niobium determines the amount of liquid formed and the extent of template growth. The amount of excess Nb required for grain growth can be reduced to ~500 ppm. X-ray diffraction measurements and dielectric property measurements confirm the biaxial texture anisotropy of  $\text{Sr}_2\text{Nb}_2\text{O}_7$  produced by TGG.

## REFERENCES

1. S. Matsuzawa and S. Mase, "Method for Producing a Single Crystal of Ferrite", US Patent 4,339,301 (1982).
2. S. Sabol, G. L. Messing and R. E. Tressler, "Textured Alumina Fibers with Elongated Grains", Hi Temp Review, NASA Publ. No. 10104, October, 1992.
3. M. Imaeda and S. Matsuzawa, "Growth of YIG Single Crystal by Solid-Solid Reaction", Proc. 1st Japan Intl SAMPE, 419-424 (1989).
4. T. Yamamoto and T. Sakuma, "Fabrication of BaTiO<sub>3</sub> Single Crystals by Solid State Grain Growth", *J. Am. Ceram. Soc.* **77** 1107-09 (1994),
5. P. W. Rehrig, S-E. Park, S. Trolier-McKinstry, G. L. Messing, B. Jones, and T. R. Shrout, "Piezoelectric Properties of Zirconium-doped Barium Titanate Single Crystals Grown by Templated Grain Growth," *J. Appl. Phys.* **86** (3):1657-1661 (1999).
6. P. W. Rehrig, G. L. Messing, and S. Trolier-McKinstry, "Templated Grain Growth of Barium Titanate Single Crystals," *J. Am. Ceram. Soc.* **83** [11] 2654-60 (2000).
7. P. Rehrig, S. Trolier-McKinstry, S.-E. Park, and G. L. Messing, "Dielectric and Electromechanical Properties of Barium Titanate Single Crystals Grown by Templated Grain Growth," *IEEE Transactions on Ultrasonics, Ferroelectrics and Frequency Control* **47** [4] 895-902 (2000)
8. S. Sabol, "Development of a Textured and Tabular Grain Microstructure via Seeded Sol Gel Processing", Ph.D. Dissertation, Pennsylvania State University (1994).
9. D. Hagelberg and D. Payne, "Grain Oriented Lithium Niobate Thin Layers Prepared by Sol Gel Methods", in *Ferroelectric Thin Films* 19-24 (1990)
10. Y. Chen, et al., "Microstructure and Superconducting Properties of YBCO Thin Films Formed by Metalorganic Deposition", *J. Mater Res.*, **4** [5] 1065-1081 (1989)
11. U. Selvaraj, A.V. Prasadaraao, S. Komarneni and R. Roy, "Epitaxial or Oriented Crystallization of Chemically Modified Sol-Gel TiO<sub>2</sub> Thin Films," *J. Am. Ceram. Soc.* **75** [5] 1378 (1992).
12. K. Miller, C. Chan, M. Cain and F. Lange, "Epitaxial Zirconia Thin Films from Aqueous Precursors", *J. Matl Res.*, **8** [1] 169-177 (1993).
13. A. Fouskova and L. E. Cross, "Dielectric Properities of Bismuth Titanate," *J. Appl. Phys.*, **41**, 2834-2838 (1970).
14. S. E. Cummins and L. E. Cross, "Electrical and Optical Properties of Ferroelectric Bi<sub>4</sub>Ti<sub>3</sub>O<sub>12</sub> Single Crystals," *J. Appl. Phys.*, **39** [5], 2268-2274 (1968).
15. V. K. Seth, W. A. Schulze, "Grain-oriented Fabrication of Bismuth Titanate Ceramic and Its Electrical Properties," *IEEE Trans. Ultrasonics, Ferroelectrics, and Frequency Control*, **36**, 41-49, (1989).

16. T. Takenaka and K. Sakata, "Grain Orientation and Electrical Properties of Hot-forged  $\text{Bi}_4\text{Ti}_3\text{O}_{12}$  Ceramics," *Jap. J. Appl. Phys.*, **19**, 31-39 (1980).
17. H. Watanabe, T. Kimura, and T. Yamaguchi, "Sintering of Platelike Bismuth Titanate Powder Compacts with Preferred Orientation," *J. Am. Cer. Soc.*, **74**, 139-147, (1991).
18. B. Brahmaroutu, G. L. Messing, S. Trolier-McKinstry and U. Selvaraj, "Templated Grain Growth of Textured  $\text{Sr}_2\text{Nb}_2\text{O}_7$ ," Proceedings of the Tenth IEEE International Symposium on Applications of Ferroelectrics Vol II. edited by B. M. Kulwicki, A. Amin and A Safari, IEEE, Piscataway, NJ 883-886 (1996).
19. J. Horn, S. C. Zhang, U. Selvaraj, G. L. Messing, S. Trolier-McKinstry, M. Yokoyama, "Fabrication of Textured  $\text{Bi}_4\text{Ti}_3\text{O}_{12}$  by Templated Grain Growth," Proceedings of the Tenth IEEE International Symposium on Applications of Ferroelectrics Vol II. edited by B. M. Kulwicki, A. Amin and A Safari, IEEE, Piscataway, NJ 943-946 (1996).
20. P. A. Fuierer, "Grain Oriented Perovskite Layer Structure Ceramics For High Temperature Piezoelectric Applications," Ph.D. Thesis, Pennsylvania State University (1991).
21. J. A. Horn, S. C. Zhang, U. Selvaraj, G. L. Messing, and S. Trolier-McKinstry, "Templated Grain Growth of Textured Bismuth Titanate," *J. Am. Ceram. Soc.* **82**[4] 921-26 (1999).
22. S. S. Lopatin, T. G. Lupeiko, T. L. Vasiltsova, N. I. Basenko, and I. M. Berlizev, "Properties of Bismuth Titanate Ceramics Modified with Group V and VI Elements," *Inorg. Mater.*, **24**, 1328-31 (1988).
23. S. K. Kim, M. Miyayama, and H. Yanagida, "Electrical Anisotropy and A Plausible Explanation for Dielectric Anomaly  $\text{Bi}_4\text{Ti}_3\text{O}_{12}$  Single Crystals," *Mat. Res. Bull.*, **31**(1) 121-31 (1996).
24. H. S. Shulman, M. Testorf, D. Damjanovic, and N. Setter, "Microstructure, Electrical Conductivity, and Piezoelectrical Properties of Bismuth Titanate," *J. Am. Ceram. Soc.*, **79**[12] 3124-28 (1996).
25. A. Saneto and L. E. Cross, "Electro-mechanical Behavior of Single Domain Single Crystals of Bismuth Titanate ( $\text{Bi}_4\text{Ti}_3\text{O}_{12}$ )," *J. Mater. Sci.*, **17**, 1409-12 (1982).
26. H. J. Bunge and C. Esling, Eds., Quantitative Texture Analysis, DGM Informationsgesellschaft m.b.H., Verlag, Germany (1981)
27. B. D. Cullity, Elements of X-ray Diffraction, 2<sup>nd</sup> Ed., Addison-Wesley Publ. Co., Inc., Reading, MA (1978).
28. B. Brahmaroutu, G. L. Messing, and S. Trolier-McKinstry, "Densification and Anisotropic Grain Growth in  $\text{Sr}_2\text{Nb}_2\text{O}_7$ ," *J. Mat. Sci.* **35** 5673-80 (2000).
29. P. Leshchenko, A. Shevchenko, L. Lylova, L. Kovba and E. Ippolitova, "The System  $\text{SrO-Nb}_2\text{O}_5$ ," *Russ. J. Inorg. Chem.*, **18**[7] 1202-05 (1982).

30. B. Brahmaroutu, G. L. Messing, and S. Troler-McKinstry, "Molten Salt Synthesis of Anisotropic  $\text{Sr}_2\text{Nb}_2\text{O}_7$  Particles," *J. Am. Ceram. Soc.*, **82** [6] 1566-68 (1999)
31. NIH Image, v. 1.56, by W. Rasband, National Institute of Health, USA.
32. P. Hartman and W. G. Perdok, "On the Relations between Structure and Morphology of Crystals. I," *Acta Cryst.*, **8** 49-51 (1955)
33. B. Brahmaroutou, "Templated Grain Growth of Textured Strontium Niobate Ceramics," PhD Dissertation , Pennsylvania State University, University Park, PA (1999).
34. S. Bae and S. Baik,, "Determination of Critical Concentrations of Silica and/or Calcia for Abnormal Grain Growth in Alumina," *J. Am. Ceram. Soc.*, **76** [4] 106567 (1993).

## Personnel Supported

The co-PIs for the proposed project were Professors Gary L. Messing, Professor of Ceramic Science and Engineering, and Susan Trolier-McKinstry, Associate Professor of Ceramic Science and Engineering. Bhaskar Brahmaroutou completed most of his Ph.D. studies on this project and is reported in his dissertation, "Templated Grain Growth of Textured Strontium Niobate Ceramics" in August, 1999. Two post-doctoral students, Drs. Jeffery Horn and Song Hyeon Hong worked on TGG of  $\text{Bi}_4\text{Ti}_3\text{O}_{12}$  and doped  $\text{Bi}_4\text{Ti}_3\text{O}_{12}$ , respectively.

## Publications Based on Work

1. M. Seabaugh, S. H. Hong and G. L. Messing, "Processing of Textured Ceramics by Templated Grain Growth" in Ceramic Microstructure: Control at the Atomic Level, eds. A. P. Tomsia and A. Glaeser, Plenum Press, New York, 303-310 (1998).
2. B. Brahmaroutu, G. L. Messing, S. Trolier-McKinstry and U. Selvaraj, "Templated Grain Growth of Textured  $\text{Sr}_2\text{Nb}_2\text{O}_7$ ," Proceedings of the Tenth IEEE International Symposium on Applications of Ferroelectrics Vol II. edited by B. M. Kulwicki, A. Amin and A Safari, IEEE, Piscataway, NJ 883-886 (1996).
3. J. Horn, S. C. Zhang, U. Selvaraj, G. L. Messing, S. Trolier-McKinstry, M. Yokoyama, "Fabrication of Textured  $\text{Bi}_4\text{Ti}_3\text{O}_{12}$  by Templated Grain Growth," Proceedings of the Tenth IEEE International Symposium on Applications of Ferroelectrics Vol II. edited by B. M. Kulwicki, A. Amin and A Safari, IEEE, Piscataway, NJ 943-946 (1996).
4. J. Horn, S. C. Zhang, U. Selvaraj, G. L. Messing, and S. Trolier-McKinstry, "Templated Grain Growth of Textured  $\text{Bi}_4\text{Ti}_3\text{O}_{12}$ ," J. Am. Ceram. Soc. **82**(4):921-926 (1999).
5. S-H Hong, S. Trolier-McKinstry, and G. L. Messing, "Anisotropic Dielectric and Electromechanical Properties in Textured Nb-doped Bismuth Titanate Ceramics," J. Am. Ceram. Soc. **83**(1): 113-118 (2000).
6. B. Bramaroutou, G. L. Messing and S. McKinstry, "Molten Salt Synthesis of Anisotropic SN Particles," J. Am. Ceram. Soc. **82**(6):1565-1568 (1999).
7. S-H Hong, J. A. Horn, S. Trolier-McKinstry, and G. L. Messing, "Dielectric and Ferroelectric Properties of Ta-doped Bismuth Titanate," J. Mat. Sci. Lett. **19** (18) 1661 (2000).
8. B. Brahmaroutu, G. L. Messing, and S. Trolier-McKinstry, "Densification and Anisotropic Grain Growth in  $\text{Sr}_2\text{Nb}_2\text{O}_7$ ," J. Mat. Sci. **35** 5673-80 (2000).
9. K. Watari, B. Brahmaroutu, S.-C. Cheng, G. L. Messing, and S. Trolier-McKinstry, "Epitaxial Growth of Anisotropically Shaped Single Crystal Particles of Cubic  $\text{SrTiO}_3$ ," J. Mat. Res. **15** [4] 846-849 (2000).
10. B. Brahmaroutu, G. L. Messing, and S. Trolier-McKinstry, "Biaxially Textured La-doped  $\text{Sr}_2\text{Nb}_2\text{O}_7$  Produced by Templated Grain Growth", (accepted for publication) J. Mat. Res. (2001)



11. E. M. Sabolsky, C. Duran, B. Brahmaroutu, S. Troler-McKinstry and G.L. Messing, "Textured Ferroelectric Ceramics by Templated Grain Growth with Property Anisotropy", in Ceramic Processing Science-VI, G. L. Messing, S. Hirano and N. Claussen eds., American Ceramic Society, Westerville, OH, (2001).

#### **List of US Patents**

P. W. Rehrig, S.-E. Park, T. R. Shrout, G. L. Messing, S. Troler-McKinstry, and B. Jones, "Crystallographically Engineered Perovskite Single Crystals for High Performance Piezoelectrics," invention disclosure

C. Duran, Gary L. Messing, Susan Troler-McKinstry, "Grain-oriented tungsten bronze ceramics with improved electrical properties," PSU Invention Disclosure No. 99-2089.

K. Watari, G. L. Messing, S. Troler-McKinstry, "Preparation of Anisotropic Perovskite Particles," Invention Disclosure submitted in April 1999

#### **Presentations Based on Work**

"Templated Grain Growth of Textured, High Temperature Piezoelectrics", G. L. Messing and S. Troler-McKinstry, AFOSR Ceramic Materials Contractors Conf., Hueston Woods, OH (May 23, 1995)

"Templated Grain Growth of Textured, High Temperature Piezoelectrics" G. L. Messing and S. Troler-McKinstry, ONR Workshop on Ferroelectric Single Crystals, Penn State (March 28, 1996)

"Fabrication of Textured High Temperature Piezoelectrics by Templated Grain Growth" G. L. Messing and S. Troler-McKinstry, AFOSR Program Review, Hueston Woods, OH, (May 29-30, 1995)

"Regulating Microstructure Evolution via Templated Anisotropic Grain Growth." G. L. Messing (Invited paper) Gordon Research Conference on Solid State Studies in Ceramics, Meriden, NH (August 4, 1996).

"Single Crystal-Like High Temperature Ferroelectrics by a Templated Grain Growth Approach", G. L. Messing and S. Troler-McKinstry, ONR Single Crystal Workshop, Piscataway, NJ (August 18, 1996)

"Fabrication of Textured  $\text{Bi}_4\text{Ti}_3\text{O}_{12}$  by Templated Grain Growth," S. Zhang, U. Selvaraj, M. Yokoyama, J. Horn, G. L. Messing and S. Troler-McKinstry, International Symposium on the Applications of Ferroelectrics, Piscataway, NJ (August 19-22, 1996)

"Templated Grain Growth of Textured  $\text{Sr}_2\text{Nb}_2\text{O}_7$ ," B. Brahmaroutu, U. Selvaraj, G. L. Messing and S. Troler-McKinstry, International Symposium on the Applications of Ferroelectrics, Piscataway, NJ (August 19-22, 1996).

"Anisotropic Grain Growth in  $\text{Sr}_2\text{Nb}_2\text{O}_7$ ," B. S. Brahmaroutu, G. L. Messing, S. Troler-McKinstry, presented at 1998 Annual Meeting of the American Ceramic Society.

"Templated Grain Growth of Ferroelectric Materials," B. Brahmaroutu, P. W. Rehrig, S. H. Hong, S. Troler-McKinstry, and G. L. Messing, presented at the US-Japan Seminar on Dielectrics and Piezoelectrics (1998).

"Templated Grain Growth of Perovskite Ferroelectrics," P. W. Rehrig, C. Duran, E. M. Sabolsky, S. Trolier-McKinstry, and G. L. Messing, presented at the ONR Transducer Review Meeting, University Park, PA (1998).

"Templated Grain Growth of Perovskite Ferroelectrics," P. W. Rehrig, E. M. Sabolsky, S. Trolier-McKinstry, G. L. Messing, presented at International Symposium on Applications of Ferroelectrics, Montreux, Switzerland (1998).

"Templated Grain Growth (TGG) in  $0.65\text{Pb}(\text{Mg}_{1/3}\text{Nb}_{2/3})\text{O}_3$ - $0.35\text{PbTiO}_3$ ," E. M. Sabolsky, G. L. Messing, S. Trolier-McKinstry, presented at Gordon Conference (1998).

"Templated Grain Growth for Production of Highly Textured or Single Crystal Piezoelectrics", G. L. Messing, DARPA Workshop, Washington (July 30, 1998)

"Texture Development in Alumina by Templated Grain Growth", G. L. Messing, Interface Workshop, KAIST, Taejon, Korea (Sept 17, 1998)

"Templated Grain Growth for the Fabrication of Organized Microstructures", G. L. Messing, Austceram '98 in Melbourne, Australia (Sept 29, 1998)

"Templated Grain Growth for the Fabrication of Organized Microstructures", G. L. Messing, Dept. of Materials Science and Engineering, Univ. of Michigan (Nov 6, 1998)

"Templated Grain Growth for the Fabrication of Ceramics with Organized Microstructures", G. L. Messing, Dept. of Materials Science and Engineering, Carnegie Mellon University, Pittsburgh (Jan 19, 1999)

"Ceramics with Novel Microstructure-Property Relations Produced via Templated Grain Growth", G. L. Messing, Synergy Ceramics Workshop, Osaka, Japan (Feb 4, 1999)

"Templated Grain Growth of Textured Ceramics and Single Crystals" G. L. Messing, DARPA Workshop on Solid State Crystal Growth, Arlington, VA (Feb 16, 1999)

"Fabrication of Textured Ceramics by Templated Grain Growth, G. L. Messing, Brockhouse Inst of Materials Research, McMaster University, (March 22, 1999)

"Fabrication of Textured Ceramics by Templated Grain Growth", G. L. Messing, Ohio State University, G. L. Messing, "Materials Science and Engineering Seminar (April 1, 1999)

"Textured High Temperature Piezoelectrics by Templated Grain Growth", B. Brahmaroutu, Y. Narendar, G. L. Messing and S. Trolier-McKinstry, American Ceramic Society, Indianapolis (April 25-28, 1999)

"Modeling Templated Grain Growth of Barium Titanate Single Crystals," P. Rehrig, G. L. Messing, S. Trolier-McKinstry, B. Brahmaroutu, Sintering '99 Conference, The Penn Stater Conference Hotel, November 2, 1999.

"Templated Grain Growth of Piezoelectric Ceramics," S. Trolier-McKinstry, B. Brahmaroutu, C. Duran, P. Rehrig, E. Sabolsky, and G. L. Messing, Invited presentation at the Fall 1999 MRS Meeting, Boston, MA, Nov. 29- Dec. 2, 1999.

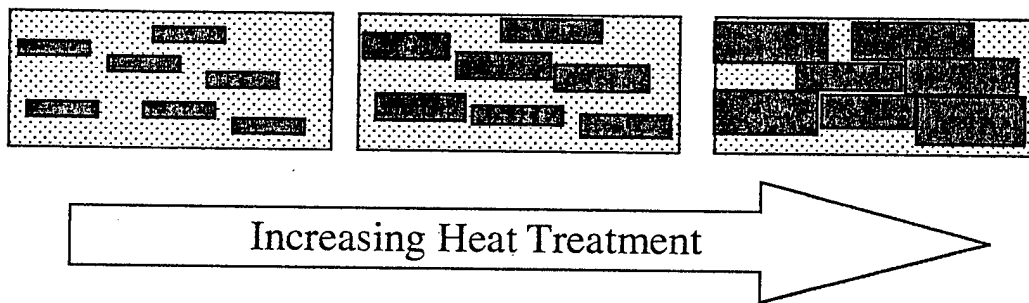


Figure 1 Schematic of the templated grain growth process.



Figure 2 Molten salt synthesized BiT platelets

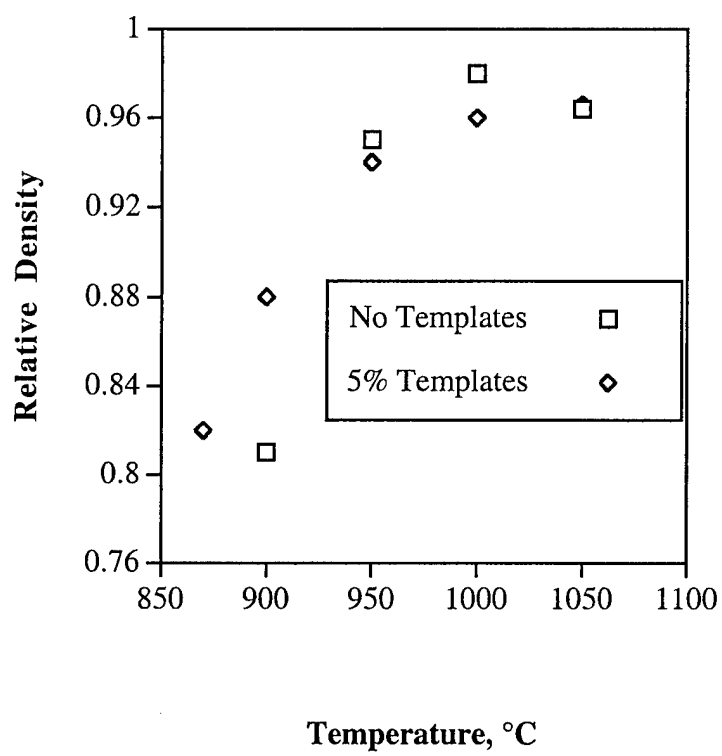


Figure 3 Effect of template particles on the densification of BiT laminates

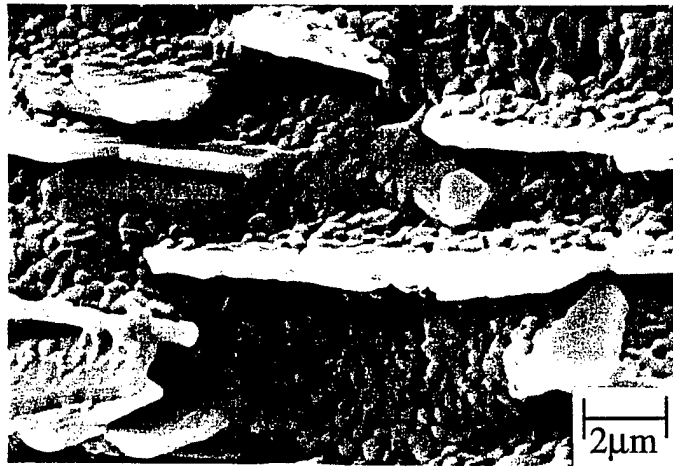


Figure 4 Edgeview of BiT laminate with 5 vol% BiT platelets sintered at 900°C for 10 min.

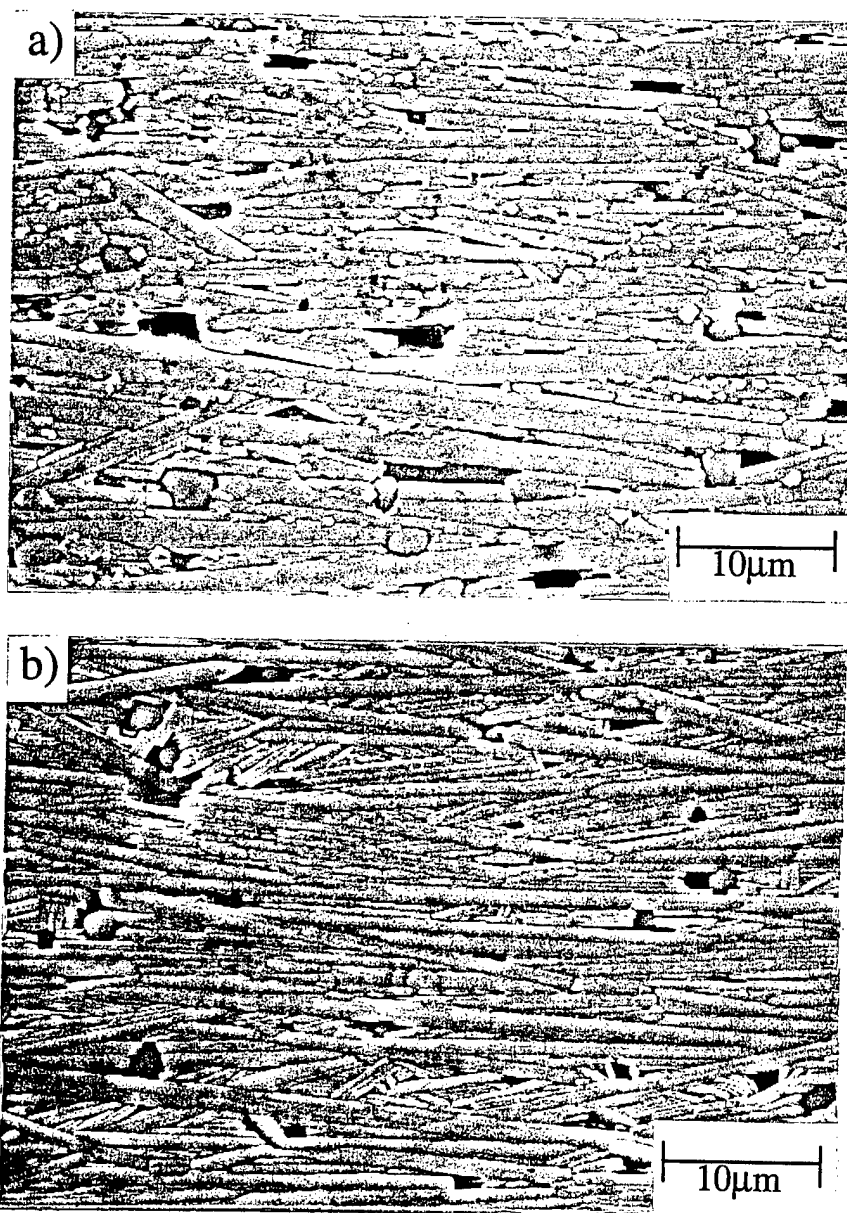


Figure 5 BiT laminates containing 5 vol% templates sintered at (a) 1000°C for 10 min and (b) 1000°C for 1 h.

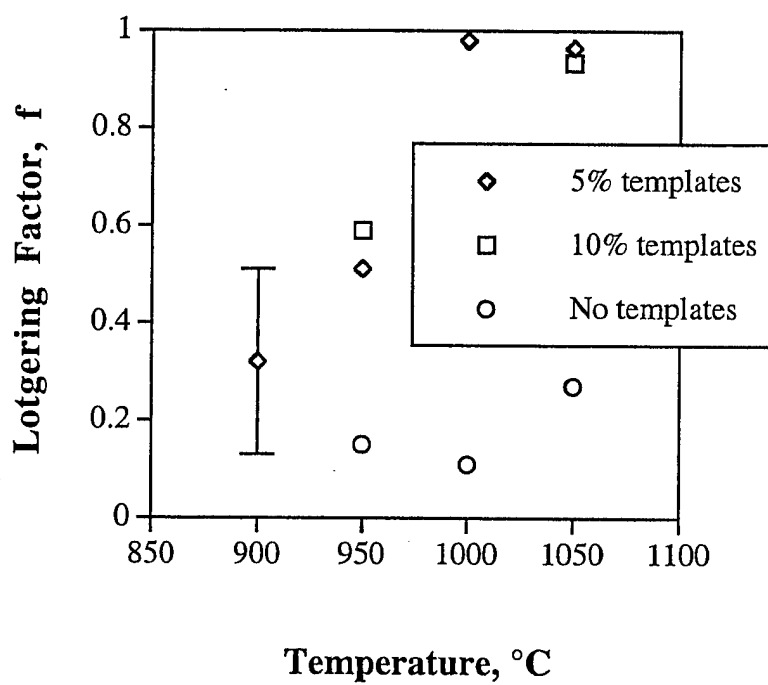


Figure 6 Effect of sintering temperature and template particles on texture development in BiT.



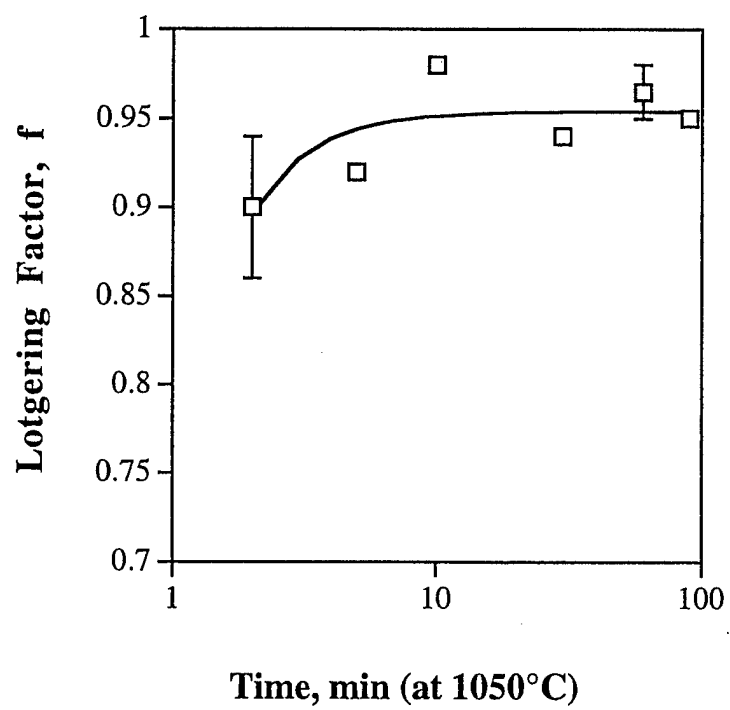


Figure 7 Effect of time on texture evolution for BiT laminates containing 5 vol% templates and heated at 1050°C

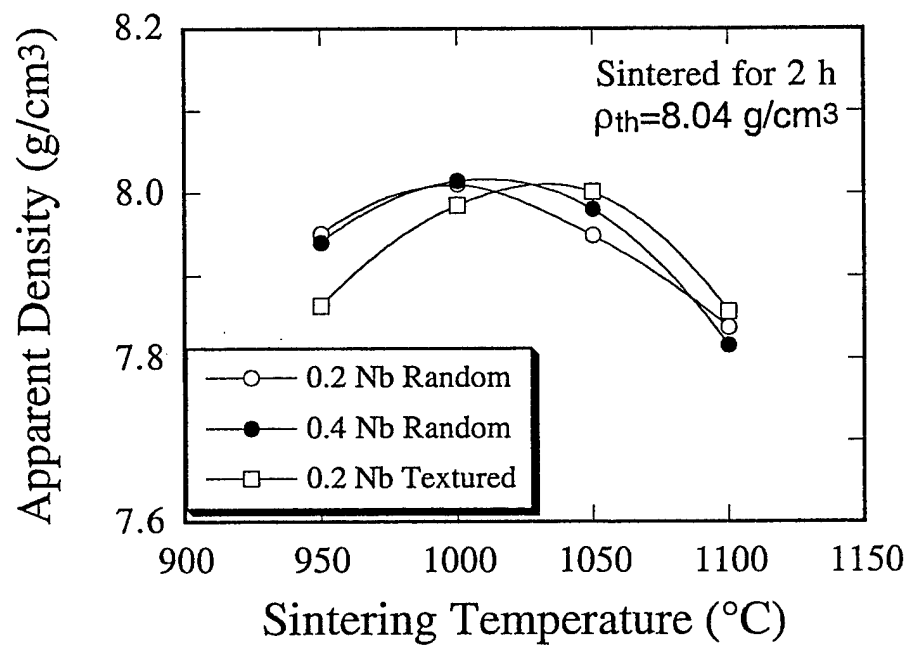


Figure 8 Apparent density of random and textured Nb-doped BiT ceramics as a function of sintering temperature.

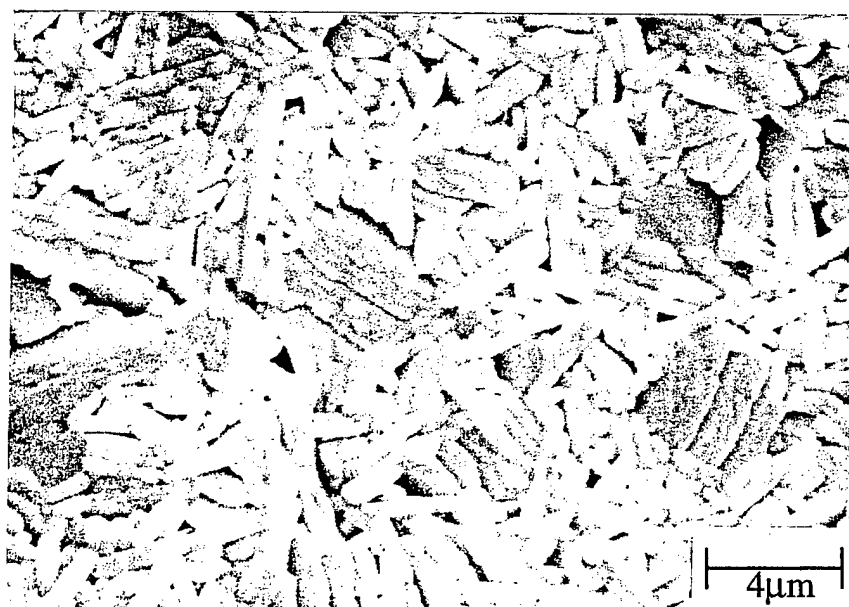
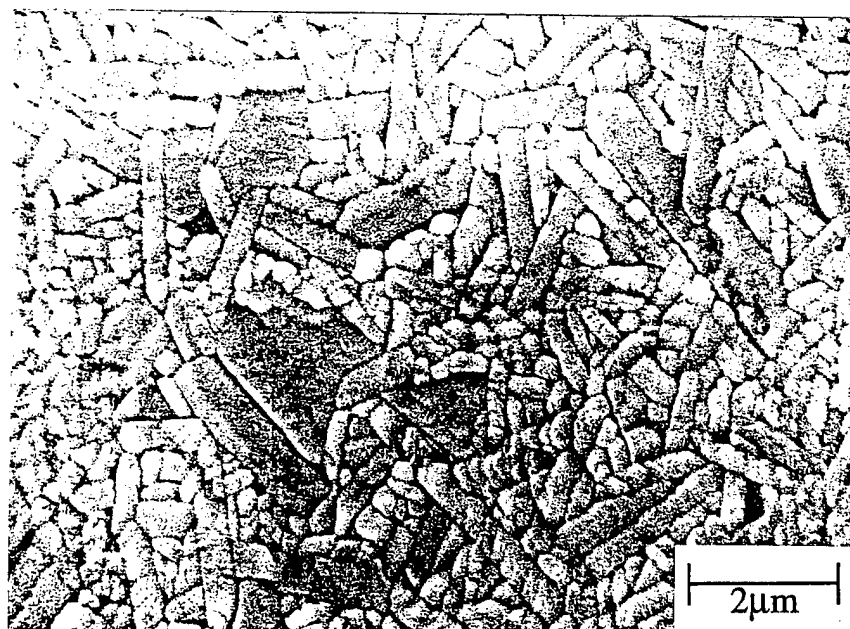


Figure 9 SEM micrographs of (top) undoped and (bottom) Nb-doped BiT ( $x = 0.2$ ) sintered at 1000°C for 2 h.

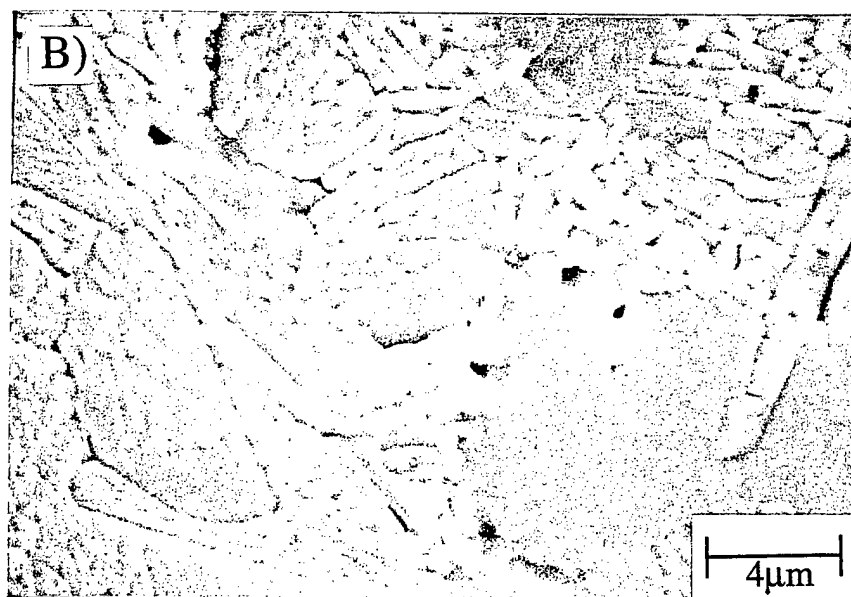
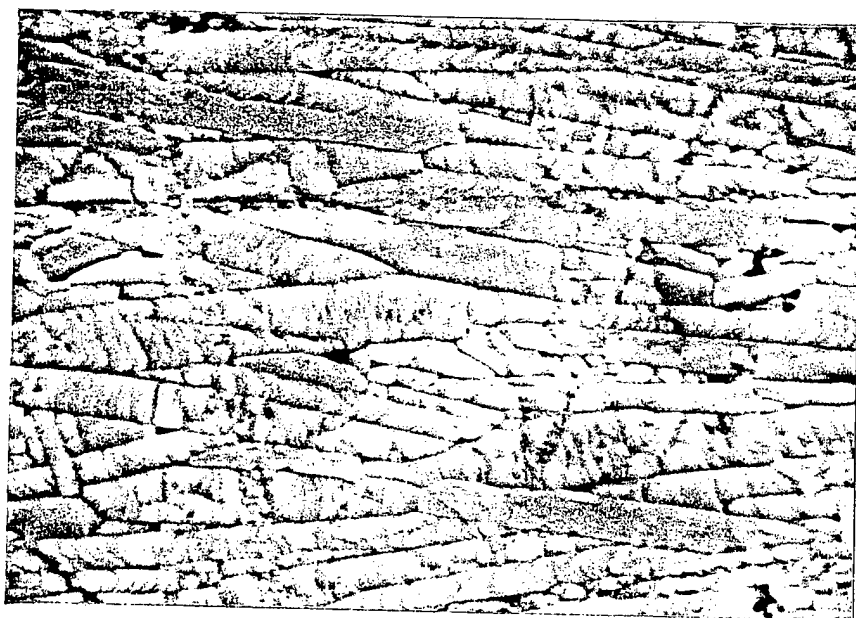


Figure 10 SEM micrographs of textured Nb-doped BiT ( $x = 0.2$ ) sintered at 1000°C for 2h, (A) cross-section and (B) top view.

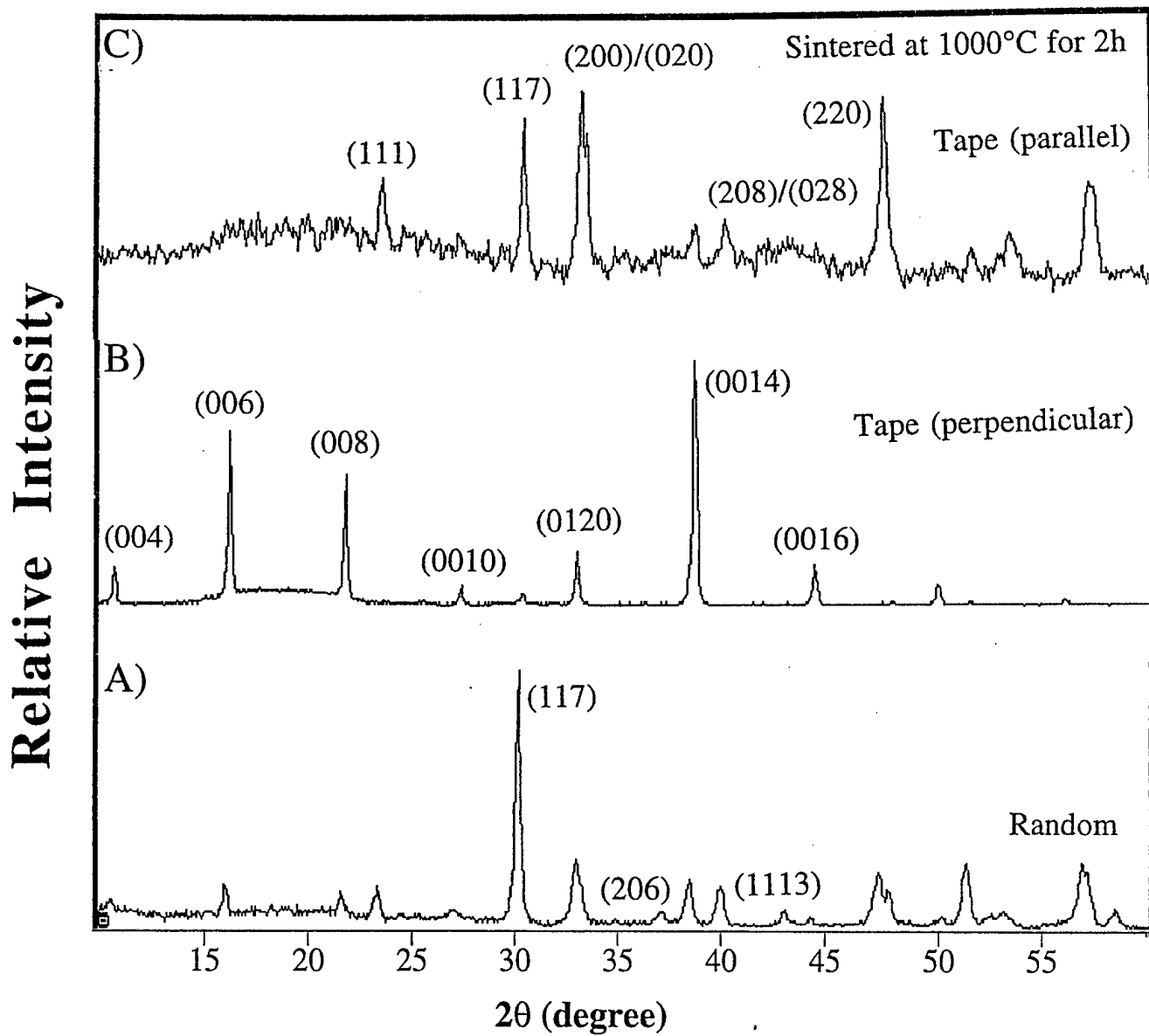


Figure 11 XRD patterns of Nb-doped BiT ( $x = 0.2$ ) sintered at  $1000^{\circ}\text{C}$  for 2 h; (A) random, (B) textured perpendicular to the casting plane and (C) textured parallel to the casting plane ( $2\theta$  scale is the same for all patterns).

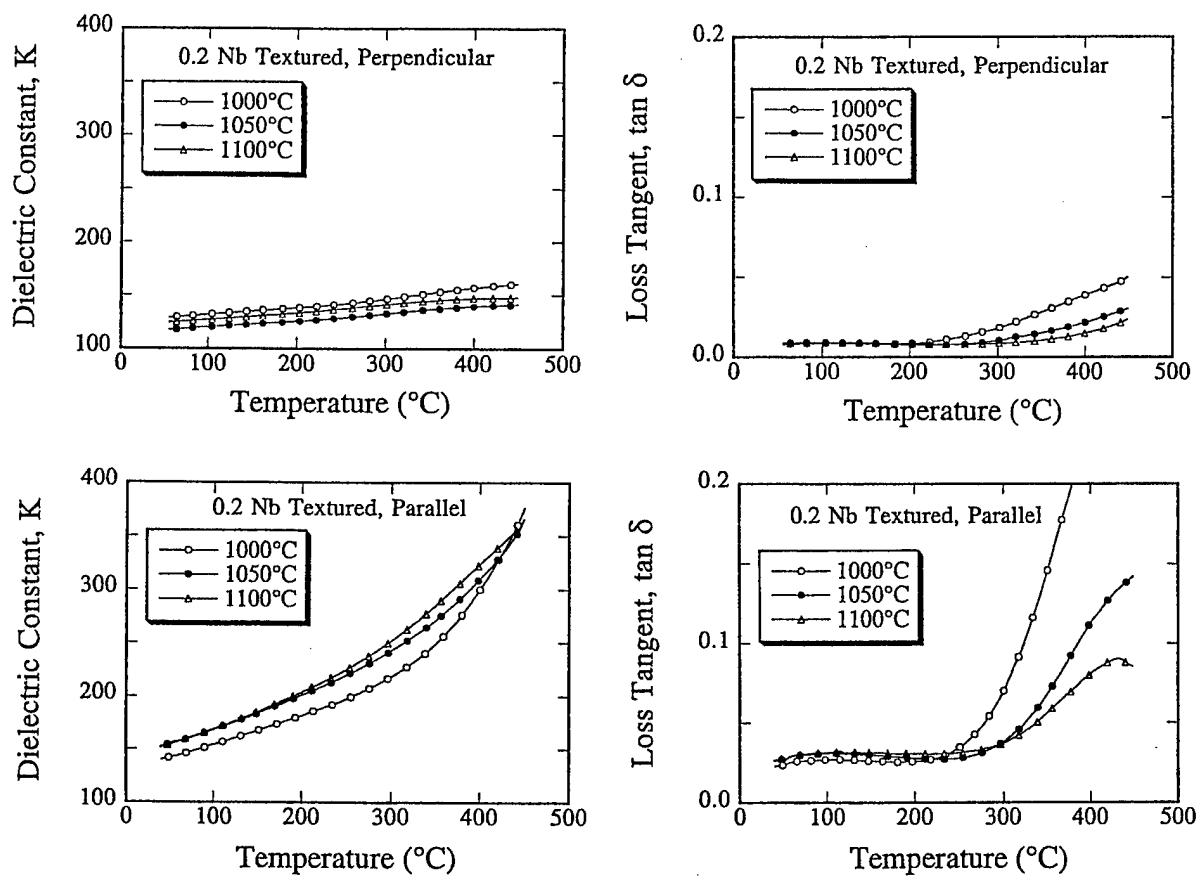


Figure 12 Dielectric constant and loss tangent at 100 Hz for textured samples sintered from 1000° to 1100°C.

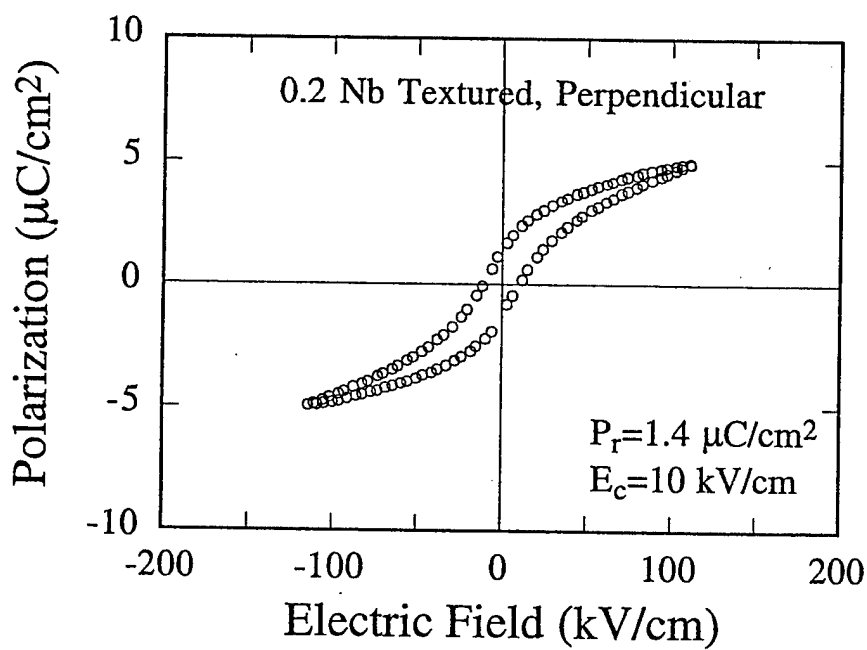
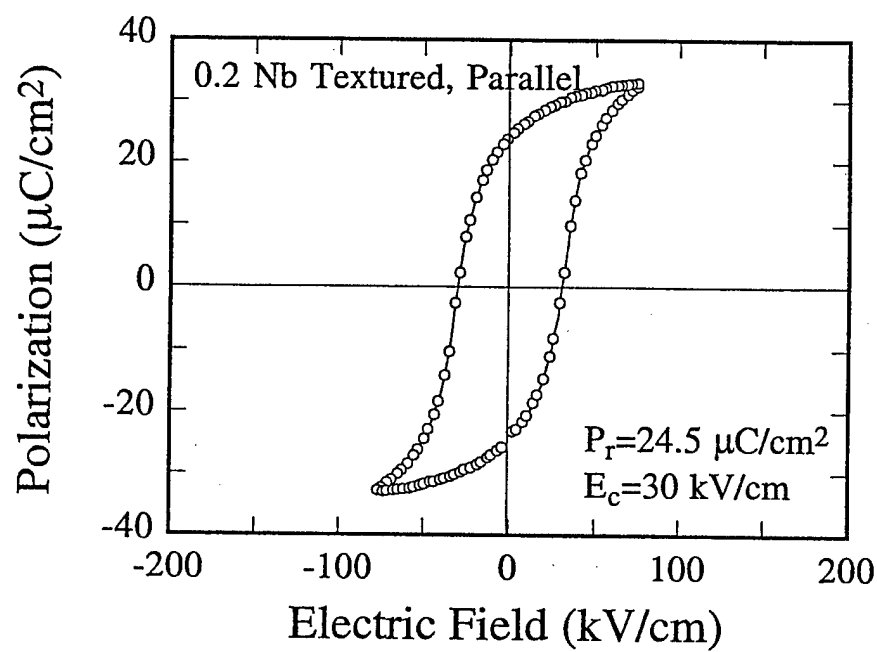


Figure 13 Hysteresis loops of textured Nb-doped BiT sintered at 1050°C for 2h.

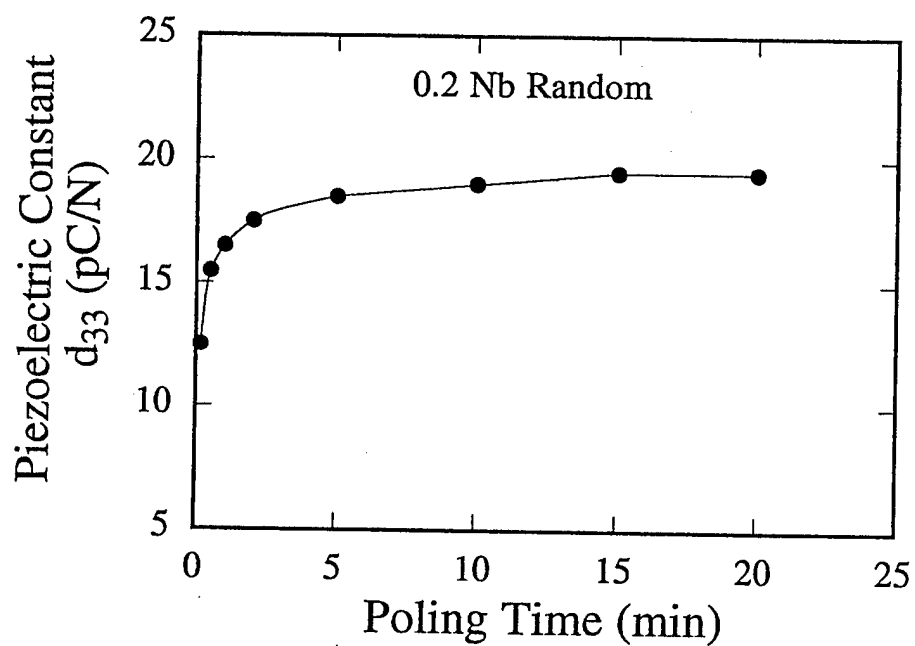


Figure 14 Variation of piezoelectric constant,  $d_{33}$ , with poling time (poling field = 70 kV/cm) in randomly oriented, Nb-doped BiT ( $x=0.2$ ) sintered at 1100°C for 2 h.



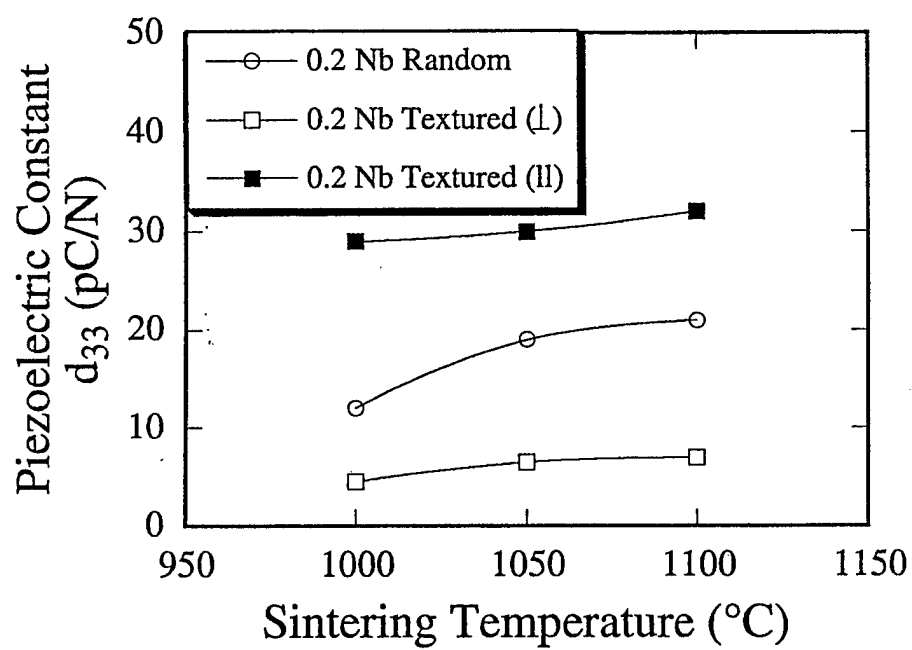


Figure 15 Piezoelectric constant,  $d_{33}$ , of random and textured Nb-doped BiT sintered for 2 h. (poling time = 15 min).

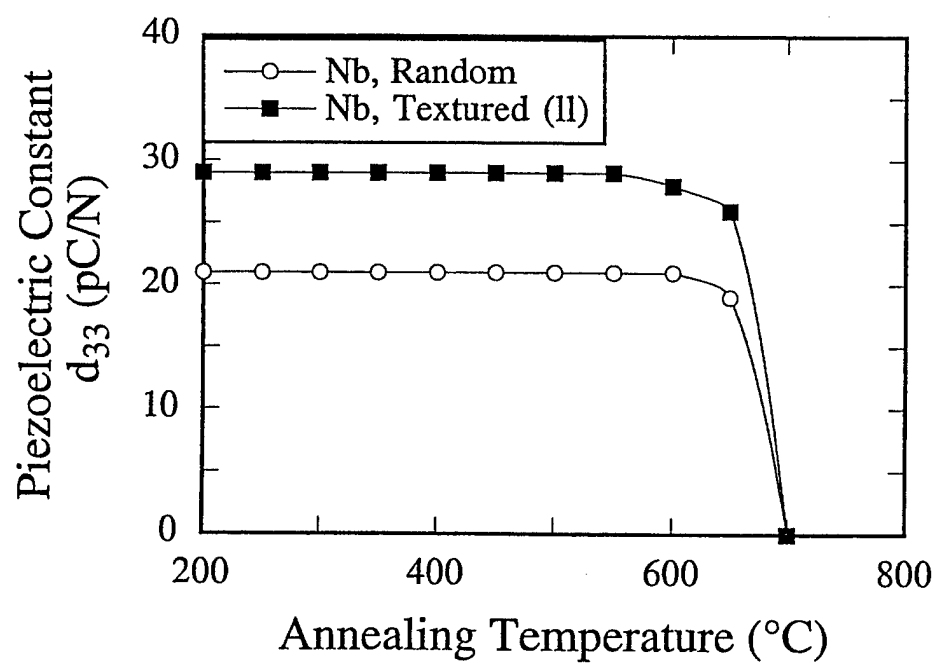


Figure 16 Effect of annealing temperature ( $t=10$  min) on the piezoelectric constants of random and textured Nb-doped BiT ( $x=0.2$ ).

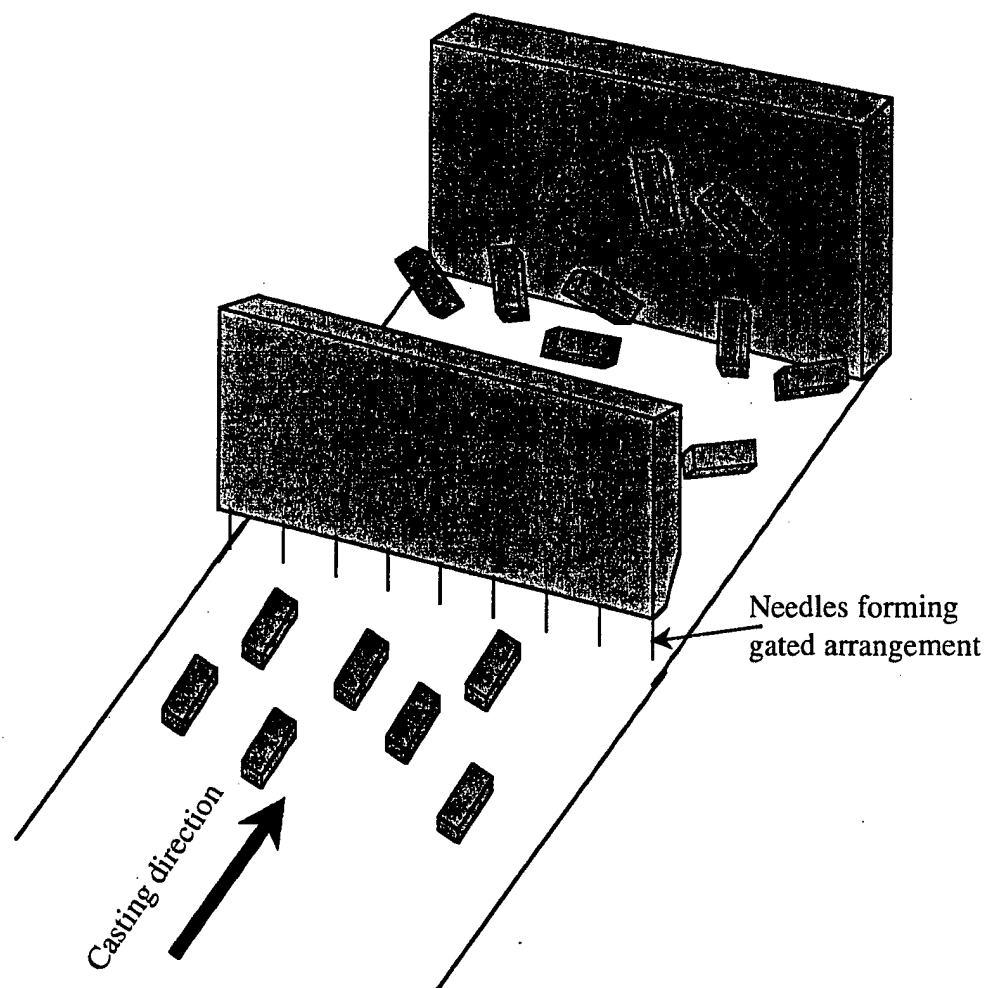


Figure 17. Gated doctor blade arrangement used for tape casting biaxially oriented samples

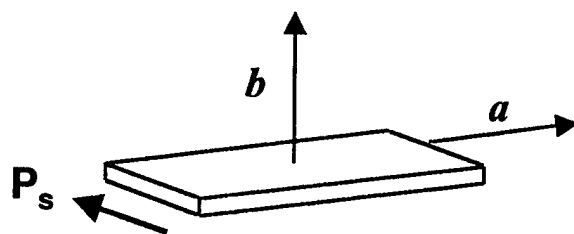
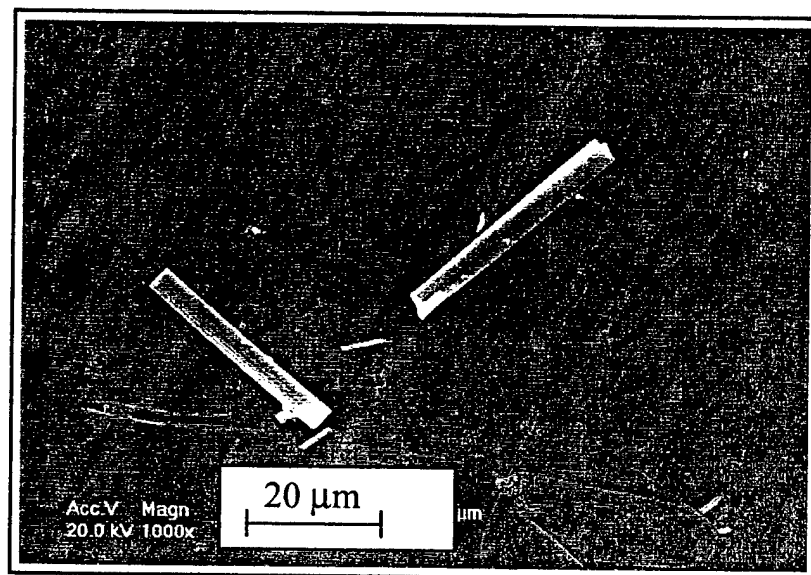


Figure 18.  $\text{Sr}_2\text{Nb}_2\text{O}_7$  template particles used to produce biaxial texture and the physical relation to crystal structure

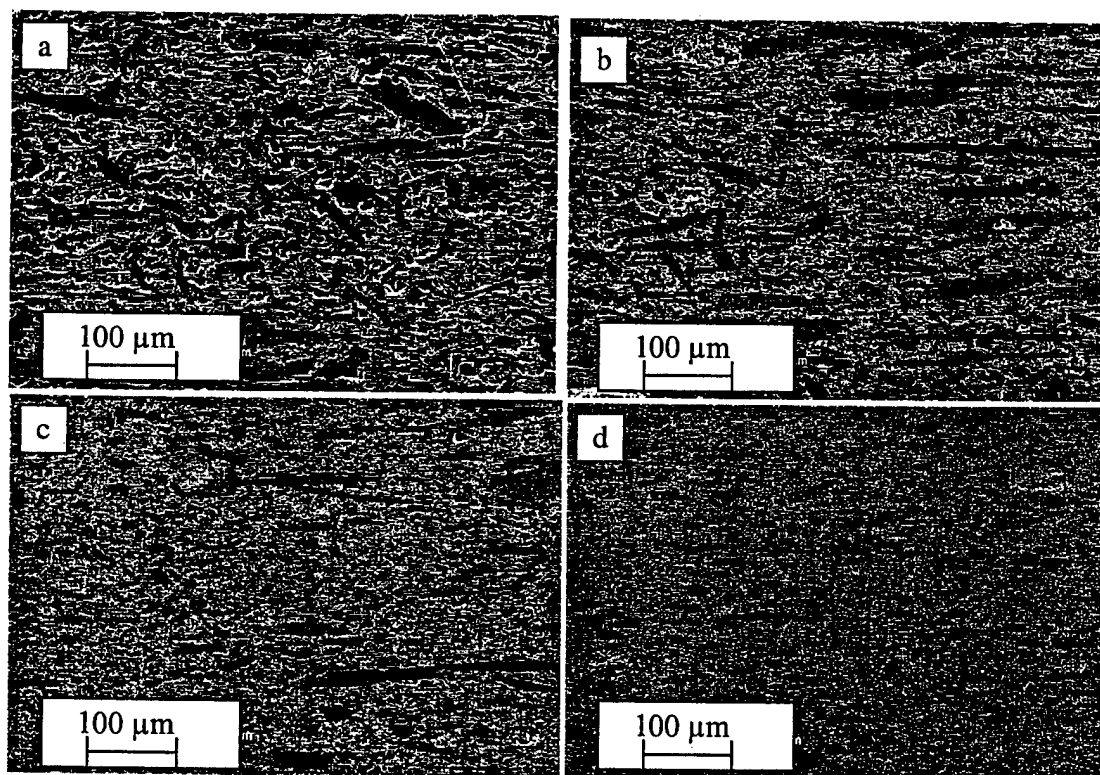


Figure 19. SEM micrographs of *c*-planes for TGG samples sintered at 1450°C for 1h (10 vol% initial templates) as a function of excess niobium (a) 1100 ppm, (b) 600 ppm, (c) 200 ppm, and (d) 20 ppm.

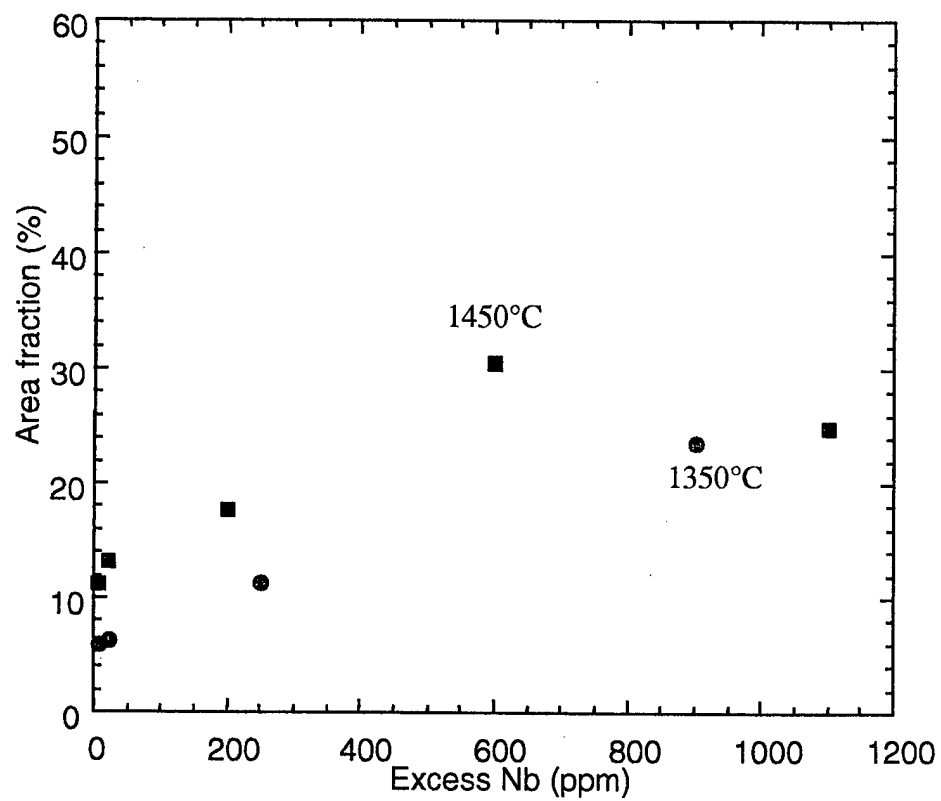


Figure 20. Area fraction occupied by a template grain as a function of excess niobium (10 vol% initial templates)

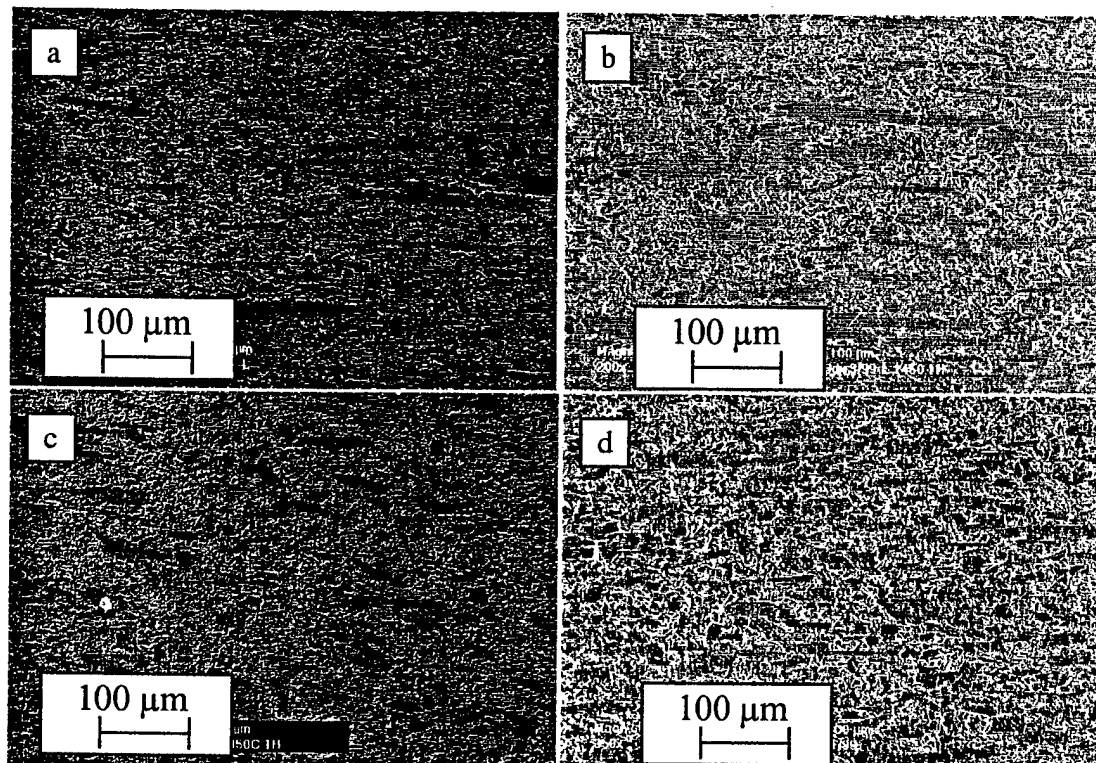


Figure 21. SEM micrographs of microstructures viewed parallel to the *c*-plane sintered at 1450°C for (a) 1 min, (b) 60 min, and parallel to the *b*-plane sintered at 1450°C for ( c) for 60 min, (d) for 120 min

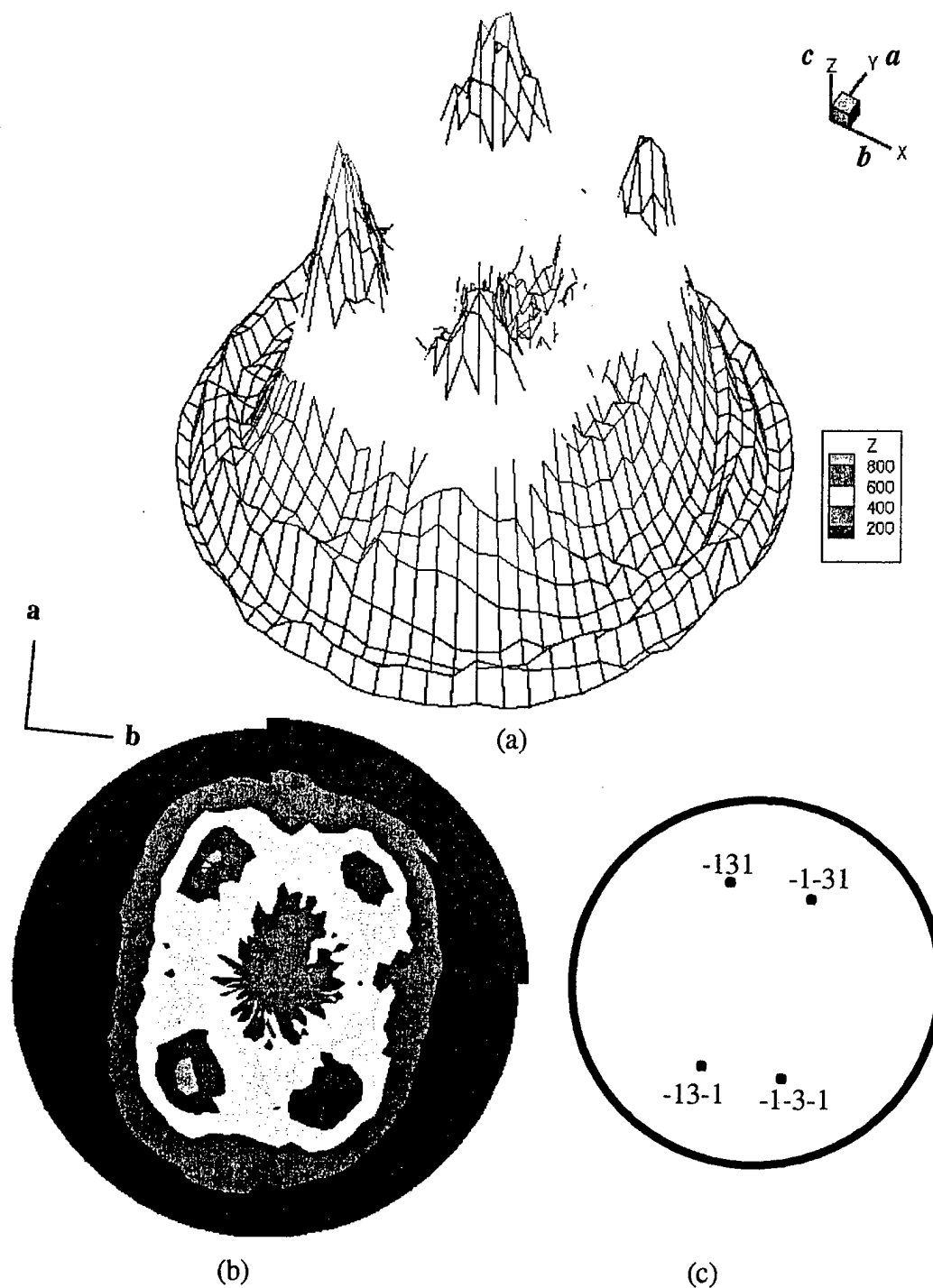


Figure 22. Pole figure from the "c" edge of biaxially textured  $(\text{Sr,La})_2\text{Nb}_2\text{O}_7$  sample showing 131 pole intensity (a) 3D representation, (b) contour plot of intensities as a function of  $\Omega$ , (c) calculated positions of 131 spots in stereographic projection on  $a$ - $b$  plane.



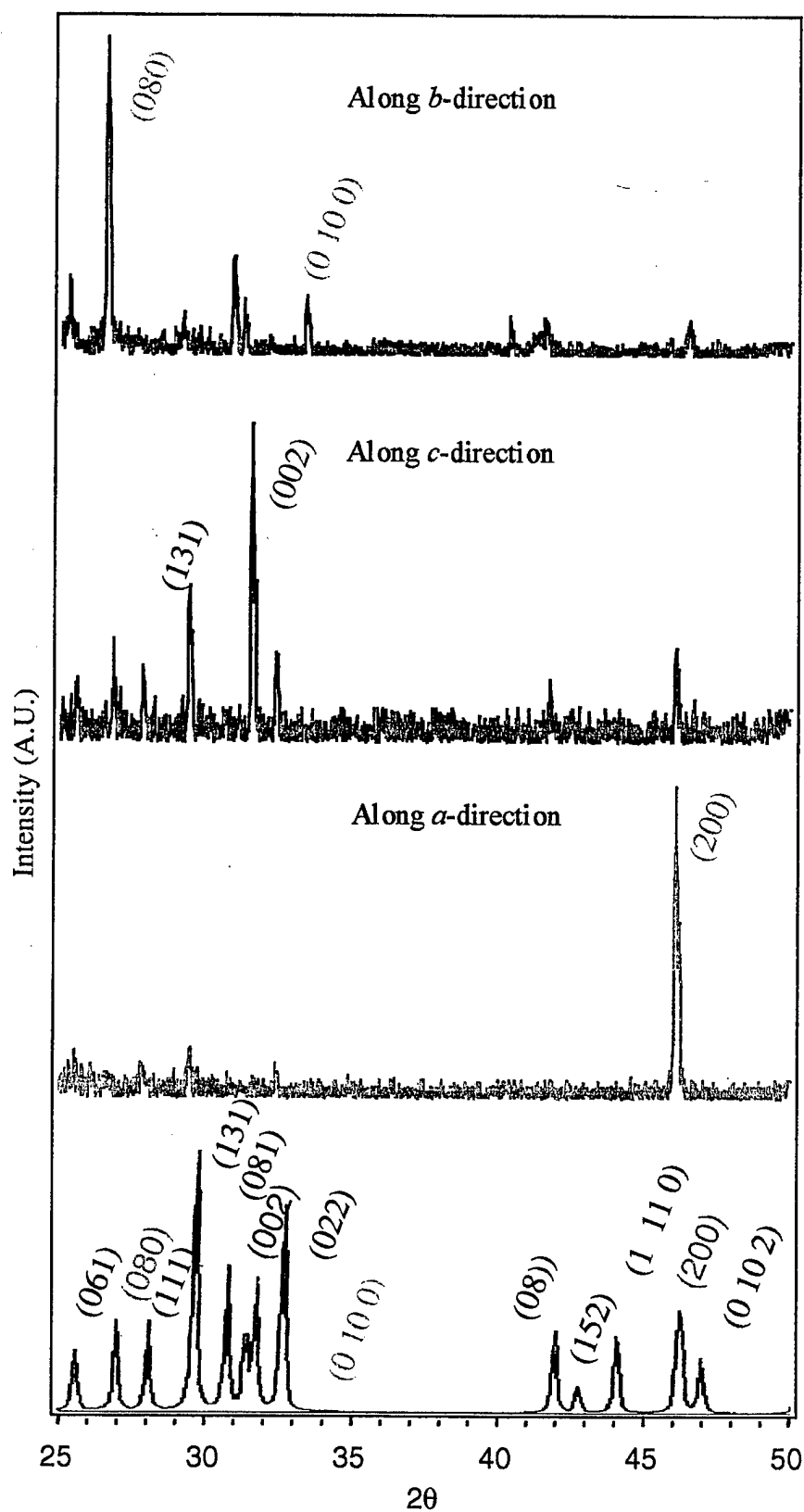


Figure 23. XRD patterns from  $a$ ,  $b$ , and  $c$ -planes for TGG samples sintered at  $1500^{\circ}\text{C}$  for 4h (10 vol% initial templates) showing biaxial texture

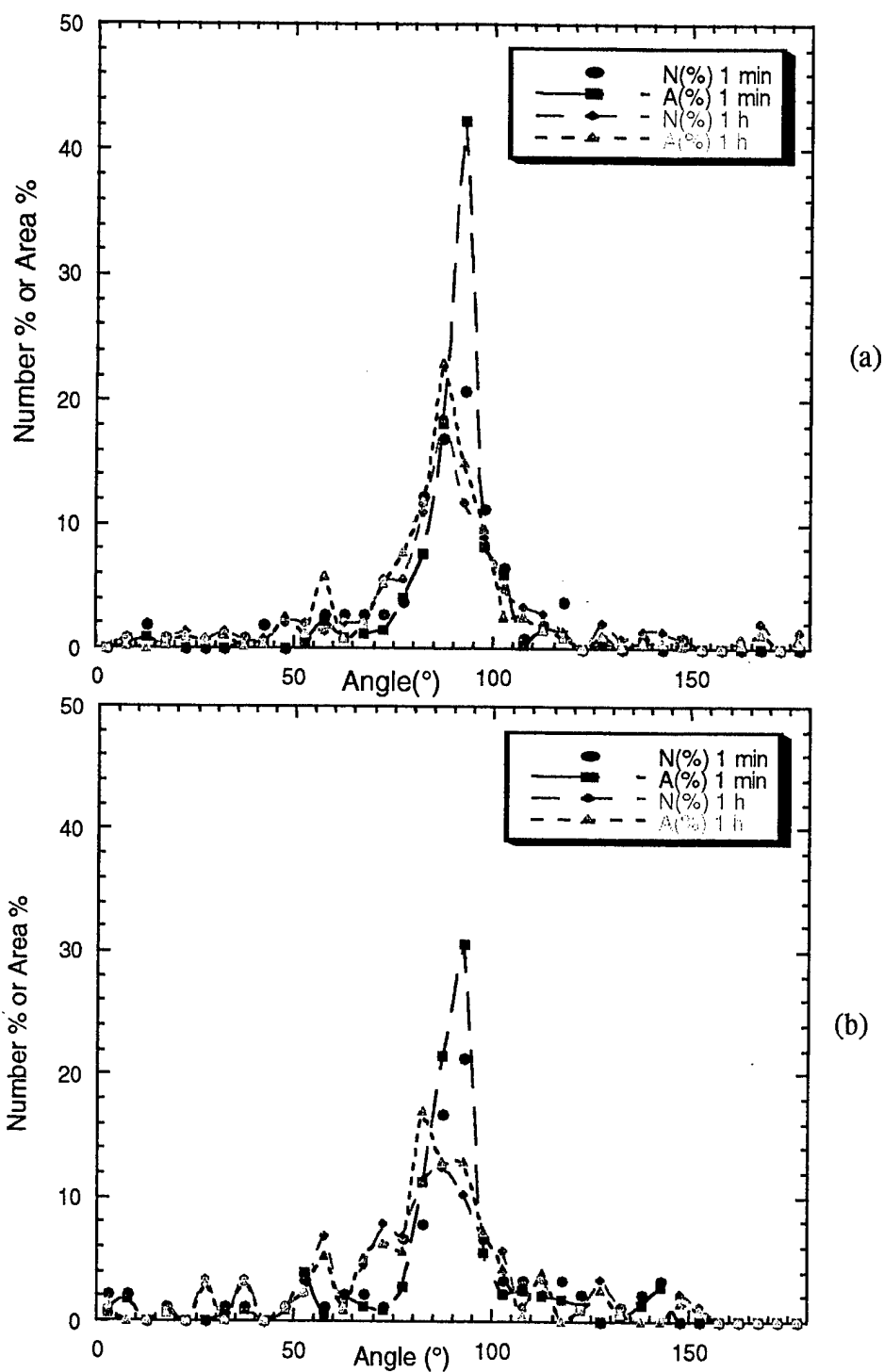


Figure 24.  $(\text{Sr,La})_2\text{Nb}_2\text{O}_7$  TGG samples (10 vol% initial templates) sintered at  $1450^\circ\text{C}$ . Number and area fraction as a function of angle from the  $b$ -axis in the (a)  $c$ -plane and (b)  $a$ -plane.  $N(\%)$  and  $A(\%)$  refer to the number percentage and area percentage of grains at a particular angle.

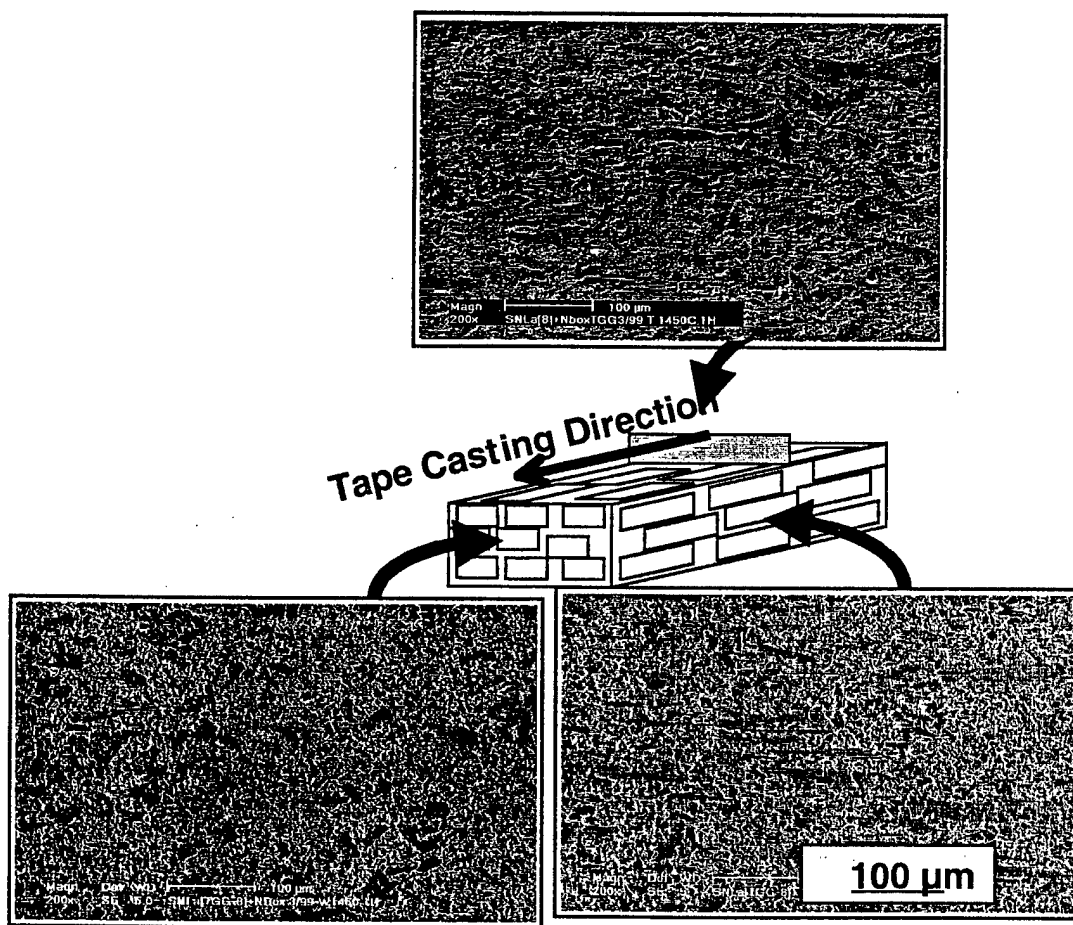


Figure 25 SEM micrographs of *a*, *b*, and *c*-planes for TGG samples sintered at 1450°C for 1 h (10 vol% initial templates) showing biaxial texture

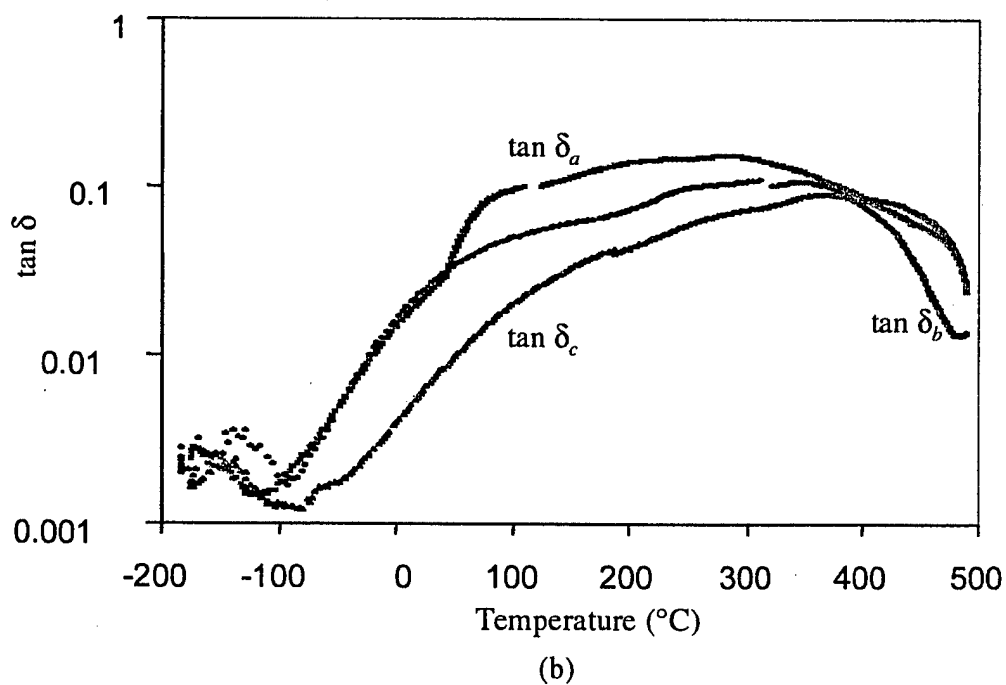
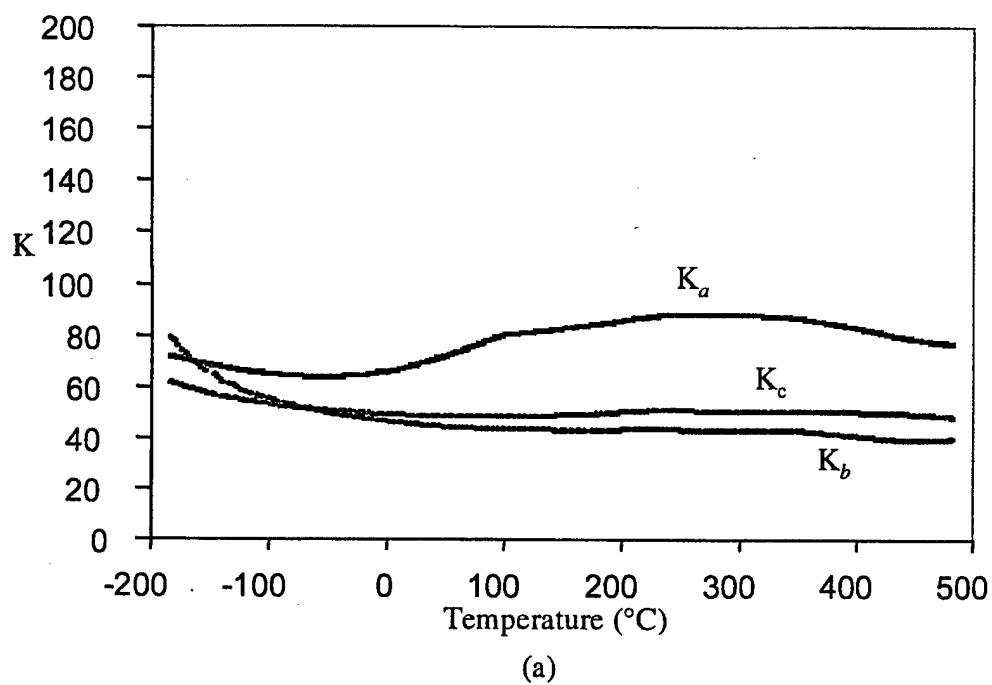


Figure 26. Dielectric properties of biaxially textured  $(\text{Sr,La})_2\text{Nb}_2\text{O}_7$  samples sintered at  $1500^\circ\text{C}$  for 4 h at 1 MHz as a function of temperature and direction (a) dielectric constant and (b) dielectric loss